R. & M. No. 3812

PROCUREMENT EXECUTIVE, MINISTRY OF DEFENCE

AERONAUTICAL RESEARCH COUNCIL
REPORTS AND MEMORANDA

A Flight Investigation of the Spanwise Lift Requirements of a Helicopter Rotor Blade

By M. J. RILEY

Structures Dept., R.A.E., Bedford

LONDON: HER MAJESTY'S STATIONERY OFFICE

1978

£4 net

A Flight Investigation of the Spanwise Lift Requirements of a Helicopter Rotor Blade

By M. J. RILEY
Structures Dept., R.A.E., Bedford

Reports and Memoranda No. 3812*
September, 1976

Summary

Surface roughness has been applied systematically to portions of the leading edge of the blades of a Wessex helicopter to reduce the local value of the maximum lift coefficient. The extent to which the inner portions of the blade could sustain a reduced maximum lift coefficient without reaching limiting control loads has been investigated. In this way, some measure of the degree to which reflex camber, with the associated small reduction in maximum lift coefficient, might be used inboard to offset the undesirable pitching moments of high performance sections nearer the blade tip, has been obtained.

In a similar way, but using local radial bands of roughness in the tip region, those areas of the blade which can provide the largest potential gain from an improved lifting capability have been identified.

* Replaces R.A.E. Technical Report 76117-A.R.C. 37 080

LIST OF CONTENTS

1. Introduction

During previous flight tests at R.A.E.[1] the effect of blade erosion on performance and blade torsional loads was investigated by artificially roughening the leading edges of the main rotor blades. In this past work the blade torsional load signature was established as a useful indicator of blade stall. The tests showed that leading edge roughness tended to initiate earlier blade stall and it was thought that its use would be a convenient way of making changes in the distribution of achievable lift coefficient along the blade. Used in this way, locally applied roughness provides an experimental tool to investigate the requirements for tailoring blade section design in order to raise the limites of rotor performance.

One of the factors which limits the performance of a rotor is blade stall on the retreating blade side of the rotor disc. Cambered sections can be used to improve the lifting ability of the blade but their large inherent pitching moments generate excessive control loads due to the high velocity on the advancing side of the rotor disc. This tends to preclude the use of highly cambered sections over the entire blade radius.

In discussion with Westland Helicopters Ltd. it was decided to investigate two aspects of this design problem. The first concerns the use of reflex cambered profiles inboard on the blade to offset the pitching moments generated by the profiles with positive camber used further outboard. The second was to explore the maximum lift coefficient requirements of the blade tip region in the complex flow field of forward flight.

Although profiles designed within the constraint of a zero or positive pitching moment requirement usually achieve a lower maximum lift coefficient than those designed to take advantage of rear loading, it was thought likely that reflex cambered profiles could be used inboard without adverse effect on the maximum performance of the helicopter. This is because, in hovering flight the inboard incidences of a normally twisted blade are below the stalling level. Also in high speed flight, inboard incidences are generally well above stall on the retreating blade, that is, in the range of azimuth that is critical for the remainder of the blade.

In the tests now described leading edge roughness was used to produce the reduction in maximum lift coefficient which might well be incurred by profiles with reflex camber. By extending the roughened regions of the blade in stages from the blade root outwards (Fig. 1) and measuring the control load levels at each stage, a point can be found at which there is a rise in the pitching moments associated with an extension of the critical areas of blade stall in high speed flight.

In the second objective, the maximum lift coefficient requirements near the tip are explored in terms of a compromise between the demands of the retreating side for more camber and greater thickness and those on the advancing side for a thin uncambered section to give less drag, less noise and smaller control loads. By choosing a roughness size which causes only a small reduction in the maximum lift coefficient, and by applying a band of roughness to the leading edge of a small length of the blade only (Fig. 1), the parts of the tip region which are most sensitive to a reduction in stalling incidence can be found from measurements of control loads as before. By implication these are the parts of the blade where the highest lifting ability is required to improve the performance of the rotor. This information can guide the choice and distribution of profile, chord length and twist to optimise performance.

The precise extent of the regions of separation on the blades is closely related to the perturbations in the downwash field caused by the trailing vortices which lie near the plane of the rotor. The resulting rapid changes of local incidence and steep radial loading gradients produce regions of separation which traverse rapidly along the blade. Two-dimensional prediction methods become inadequate in these circumstances and comprehensive wind-tunnel tests on a complete model comprising rotor and fuselage or, as described here, flight test measurements, are necessary to validate and extend rotor performance estimates.

The tests were carried out at R.A.E. Bedford during the period from September to November 1975. The *Wessex* helicopter on which the tests were made had previously completed an extensive programme of aerofoil performance testing during which an opposing pair of the blades were modified at the tip sections[2]. The roughness used in the present tests was applied to the unmodified pair of blades but the use of a non-standard rotor system is thought not to affect the conclusions drawn.

2. Flight Test Technique

2.1. The Effect of Blade Roughness and the Significance of the Control Loads

Before proceeding to describe the instrumentation and flight test techniques, it is necessary to explain in more detail how leading edge roughness causes a reduction in the maximum lift coefficient, and why measurements of the control loads can be a useful indicator of the blade performance. For the N.A.C.A. 0012 profile operating in the range of Mach numbers and Reynolds numbers found on the important parts of

the blades, the stall is of the 'trailing edge separation' type, where a turbulent boundary layer separates at a point near the trailing edge on the upper surface, and this separation point moves progressively further forward as incidence is increased towards the stall.

Leading edge roughness effectively fixes the transition point of the upper surface boundary layer very near the leading edge, and the fully turbulent boundary layer then grows to be considerably thicker at the trailing edge than if it were allowed to be laminar over part of the upper surface. Increase of the roughness size beyond that necessary to provoke transition further thickens the boundary layer and this increases the severity of the trailing edge separation. Thus the addition of leading edge roughness causes the aerofoil to stall at a lower incidence, the decrement in lift coefficient being related to the degree of roughness applied. The large and the small grit sizes used in these tests are predicted by previous flight and tunnel tests[1] to reduce the lift coefficient by approximately 20 per cent and 10 per cent respectively. Pressure measurements on the aerofoil test sections on this helicopter have also confirmed the progressive deterioration of section performance with increasing roughness.

Thus, by reducing the stalling incidence, surface roughness can increase the extent of the stalled areas of the rotor disc, and the large nose-down pitching moments generated are reflected in the control system loads. The increasingly high incidences on the retreating blade at high forward speed and the associated increase in the extent of the stalled area produce pitching moments which eventually lead to blade torsional instabilities. The strength of the control system usually defines the limit to which these torsional motions can be allowed to grow and so defines the limiting speed of the helicopter[3]. Measurement of control loads can therefore give a reliable indication of rotor performance limits.

2.2. Blade Modifications

Two of the four blades had previously been modified to make comparative performance measurements of two aerofoil sections[2]. Fairings extended over one metre of each of the tips of opposing blades and pressure sensors were housed in these fairings. One fairing was shaped to a standard N.A.C.A. 0012 profile and the other to an R.A.E. 9615 profile. It was not convenient to remove the modified blades during the present tests, but the pitch of all the blades was adjusted so that as far as possible the lift was shared equally on all four, although as a result the track of opposing pairs differed. Roughness was applied only to the standard pair of blades, and it is the behaviour of their levels of oscillatory control load which is discussed in the present report. However, the modifications are not considered likely to affect the conclusions drawn and to some extent a virtue has been made out of necessity in that the surface pressure distributions obtained on the modified blades have proved useful in the interpretation of results from the roughened blades.

2.3. Test Instrumentation

The principal parameter measured in these experiments was the blade pitch link load. Special strain-gauged links were fitted to each of the blades in place of the standard pitch change rods. In order to satisfy flight safety requirements in which a limiting pitch link load was specified, the control loads were telemetered to a ground laboratory and the aircrew advised by radio of their amplitude, particularly during the setting up of critical test conditions. On the ground, the load measurements were replayed on a pen recorder during the flight, and recorded on magnetic tape for further analysis. The same measurements were also recorded in the aircraft on a multi-channel photographic recorder together with blade bending stresses at two radial positions, blade root motions, control positions, torque and airspeed. The airborne magnetic tape recorder installed for the previous experiments was also in use during these tests to record complementary measurements of surface pressure at the tips of the two modified blades.

2.4. Test Conditions

During previous tests an extended flight envelope was permitted for this aircraft subject to monitoring of pitch link load which had resulted in an increase in permissible level flight speed and a wider variation of rotor speed. This extended envelope was again used in the present tests. Fig. 2a shows the thrust coefficient and rotational tip Mach number boundaries permitted and Fig. 2b the thrust coefficient and advance ratio boundaries defined by the extended clearance. The measured control load boundaries which effectively limit the speed of the aircraft in level flight with unroughened blades have been added and the strong dependence of these boundaries on the rotational tip Mach number can be seen.

In planning the tests to identify the parts of the blade where the incidence is high enough to be critical in respect of control loads, the programme was devised as far as practicable to evaluate separately the effects of

thrust co-efficient, Mach number and advance ratio, with a requirement for the last to be as high as possible so that realistic projections for future high performance helicopters could be made.

A further important consideration was that the range of rotor disc incidence should be comparable with future designs since the radial loading distribution depends not only on the speed of the helicopter but also on the rotor disc incidence, which in turn is determined by the magnitude of the drag of the helicopter.

As the rotor disc is tilted forward to provide a propulsive force collective pitch is applied to off-set the reductions in blade incidence caused by the component of the mean flow down through the rotor disc. However, simple vector addition of the components of the flow velocity relative to the blade shows that the inflow reduces local blade incidences to an increasingly greater extent towards the blade root, whereas the cyclic and collective pitch changes, applied to trim the rotor for a forward tilt of the disc, increase blade pitch equally at all radial positions. Hence, for a helicopter with a large drag the retreating blade tip regions have relatively high incidences and are required to generate a larger share of the lift.

The *Wessex* helicopter has a fuselage drag which must be considered high by present day design standards, and is certainly not representative of projected future designs. In order that more representative rotor load distributions be included in the present tests it was decided to employ the simple expedient of flying descending flight paths so that a component of the aircraft's weight provides a force in the flight direction to partially off-set the high drag of the fuselage. Thus, rotor loads measured in descending flight can be used to predict the loading action in level flight associated with a similarly rotored helicopter but having a reduced fuselage or parasite drag. This technique has the added advantage that the speed range of the tests could be extended beyond the level flight power limits which would normally be met in a Mk. I *Wessex*. The rate of descent and rotor disc incidence necessary to achieve a chosen value of 'equivalent drag' is calculated in the Appendix, and the results are given in Fig. 3. The range of equivalent drag chosen covers that of the standard *Wessex* helicopter down to a value representative of projected high speed helicopters, and the curves show how this wide range can be simulated by fairly moderate rates of descent within the range of speed available,

The way in which the load is redistributed along the blade is shown in Fig. 4 for blade azimuth angles of 180 degrees and 270 degrees. These local incidences are calculated using a simplified mathematical model to account for the downwash velocities, and so they are not intended to be an accurate representation of the radial loading distribution, nor can they demonstrate the increasingly large local flow perturbation due to the wake interaction as the disc tilt is reduced in descents. They do, however, illustrate well the mean incidence changes which are directly attributable to disc angle variations. They show how with increasing rate of descent, the incidences increase at inboard positions on the blade (e.g. 0·4 radius), and the incidences are reduced near the tip. Total rotor thrust is the same for all these conditions.

3. Method of Analysis

The control load waveforms are very varied, even for the limited range of steady flight conditions considered, that is, straight level flight and straight descending flight. For these flight conditions, the rotor loadings are a function of the condition of the blades (*i.e.* the leading edge roughness to be tested) and the following parameters:

Advance ratio
Rotor disc angle (rate of descent)
Rotor thrust coefficient
Mach number
Reynolds number
Ratio of blade elastic to inertia forces

In these tests, the main body of the measurements has been made keeping the rotor thrust coefficient and the rotational tip Mach number constant with sample test conditions to explore variations of these quantities. Reynolds number and the ratio of blade elastic to inertia forces could not be kept constant within the constraints so far applied, but their variation was small for all the conditions flown. Thus the control loads have been normalised by dividing by $\sigma\omega^2$ and presented as functions of blade roughness state, rotor advance ratio and rotor disc incidence, (in practical terms, rate of descent).

The disturbances to the control system arise from the aerodynamic pitching moments generated by the stalled areas of the blade. Roughness applied locally can increase the extent of these stalled areas, but to understand the effects of each roughness configuration tested it is necessary to consider first the incidence distribution at the rotor disc, and the local perturbations caused by the concentrated vorticity in the wake.

Fig, 5a shows incidence contours for a forward flight speed in the range of interest. They are derived from measurements on an *S58* helicopter[4] which has the same rotor system as the *Wessex*. Note that on the retreating blade side and around the front of the rotor disc it is the inboard portions of the blade which are at high incidence, and these are the regions which will stall first as speed is increased. 'Uniform inflow' theories do not predict this distribution. Locally high values of downwash associated with the trailing vortex system have a powerful effect on the incidence distribution and Fig. 5b shows a diagram of the vortices trailing from the blade tip for the same advance ratio. This diagram is based on the assumption that the tip vortices are simply convected downstream at the flight speed, so the tip vortex lines have an extended cycloidal shape.

Note in Fig. 5b that at $\psi = 180°$ the preceding blade's vortex crosses the blade at approximately 0·5 radius. The velocity field of this vortex plays an important part in determining the effects of roughness applied inboard on the blade. Similarly around $\psi = 360°$, the succession of trailing vortices from the other blades can combine to produce high incidences near the blade tip, and give rise to severe disturbances in the control system when tip regions of the blade are roughened.

The blade/vortex crossing points for all combinations of blade and vortex are shown in Fig. 6a for an advance ratio of 0.3. It must be remembered, however, that vortices lying just outside the disc area can have a strong effect on the incidence distributions near the tip even though the blade does not cross their paths. Clearly, these crossing positions are very dependent on the advance ratio, and in Fig. 6b the radial and azimuth locations of the crossing with the previous blade's vortex are shown for a range of advance ratios. These diagrams provide a basis for the interpretation of the control load disturbances throughout the speed range. The magnitude of the incidence increments attributable to these vortex interactions must depend on the vertical location of the vortex relative to the plane of the rotor. Estimates indicate that for the examples discussed the incidence increments are significant.

The measured control load waveforms can be interpreted more easily if they are viewed as the addition of several different disturbances to the control system. Three distinct features can be identified after examining the many differing control load waveforms, and each can be associated with blade stall at a given radial position, and at a given azimuth angle. These distinctions are arbitrarily defined for the purpose of interpreting the waveforms more easily, and indeed, as different rotor thrust coefficients and advance ratios are investigated, it will be seen how one 'feature' can merge continuously into another.

(a) Retreating blade oscillatory disturbance

For the unroughened blades the control load limit is eventually reached when the blade stall gives rise to oscillatory loads, occurring at the frequency of the first torsional mode, as the blade traverses the retreating side of the rotor disc. The azimuth position of the onset of the disturbance and its rate of growth depend on advance ratio and thrust coefficient but usually several cycles of the oscillation are present, gradually growing in amplitude, before the motion is abruptly damped around azimuth zero. This type of disturbance is also characteristic of blades roughened in the 0·80 to 0·90 radius region, as well as the unroughened blades.

(b) Disturbance at front of rotor disc

For blade roughness configurations where the blade is roughened inboard, a disturbance due to blade stall not normally found on the *Wessex* helicopter, appears around the front of the rotor disc, at around 180 degrees azimuth. It takes the form of an isolated nose-down disturbance to the blade, but does not start a persistent oscillation. The advance ratio for the onset of this disturbance correlates with the vortex crossing at $\psi = 180°$, which was identified in Fig. 5.

(c) Disturbance at rear of rotor disc

A third feature which may be distinguished is a rapid onset of the blade torsional oscillatory load late in the azimuth cycle. Although this is really a special case of the general torsional oscillation of the retreating blade, it is distinguished by its rapid growth to a large amplitude within one cycle. This disturbance is evident in conditions where roughness is applied near the extreme tip region of the blade, and may be associated with the stall in this region brought on by the combination of this roughness and the high blade incidences induced by wake interaction (see Fig. 5).

These three characteristic features are used extensively in the following discussion of the complex control load waveforms which vary considerably throughout the wide range of flight conditions and configurations of blade roughness tested.

4. Presentation and Interpretation of Control Load Measurements

4.1. Control Load Criteria and Grouping of Measurements

The quantity used to define the magnitude of the control loads is the peak-to-peak value of the oscillatory load in the pitch link, that is the difference between maximum and minimum load in any one revolution averaged over several revolutions of the rotor. Variations in the mean load were small and of little consequence when considering the fatigue strength of the control system. An oscillatory load limit of 3·11 *kN* (700 *lb*) was chosen, this value being the loading level which corresponded to an infinite fatigue life of the special pitch links fitted to this aircraft. The standard aircraft is limited by the loads in another part of the control system, resulting in flight limitations which are generally not far removed from the present criteria, since the rate of rise of control loads with speed is very rapid as the limiting conditions are approached. The control load measurements used are those recorded from the pitch link on one of the pair of roughened blades, the results from each being virtually identical.

To enable overall comparisons between the control load levels to be made more easily the results are arranged to show the datum control load levels with smooth blades first (Fig. 7) followed by the effect of roughening the blades on the level flight control loads (Fig. 8). Finally the variation of the loads with descent rate are shown for the different roughness configurations in Fig. 9. In section 4.5 these control load levels are interpreted in terms of the three characteristic waveforms already described.

4.2. Datum Results with Unroughened Blades

The control loads obtained with unroughened blades are plotted in Fig. 7 and provide a datum by which to compare results obtained with roughened blades. In the first part of this experiment, where the roughness was gradually extended in stages from the blade root, a rotor thrust coefficient of 0·0853 and a rotational tip Mach number of 0·588 were chosen as standard conditions, to enable close comparisons to be made with the previous blade roughness experiments on this aircraft. Load levels for these conditions are plotted in Fig. 7a. For the assessment of the blade lifting requirements in the tip region where roughness was in bands covering 5 per cent of the blade radius at a time, measurements were made at the same thrust coefficient but at a rotational tip Mach number of 0·547 to allow a larger range of advance ratio to be investigated. The unroughened blade results for these conditions are shown in Fig. 7b.

In each graph, a family of curves of control load versus advance ratio is plotted, each for a given descent rate. To clarify differences the zero position of the advance ratio scale is progressively shifted to the right of the page as rate of descent is increased. The horizontal scale defines this zero shift. Each curve indicates a rise in control load as forward speed is increased and comparisons between (a) and (b) reveal the sensitivity to Mach number.

The dashed lines which join points having the same advance ratio show the trend with rate of descent most clearly. With unroughened blades the control loads are only weakly dependent on rate of descent for most of this range of advance ratio, but at the highest values of advance ratio, when stall occurs on the tip region, increasing the rate of descent (which reduces the rotor disc incidence) reduces the value of oscillatory control load as expected from theoretical considerations discussed in Section 3. Although the number of measurements at the higher values of advance ratio is necessarily limited, the trends shown are well supported by results taken during minor excursions about the trim speed during the present tests, and by data obtained in previous flight tests with this aircraft.

4.3. Effect of Roughness on Loads in Level Flight

The peak-to-peak values of the control loads measured for each extent of leading edge roughness are plotted in Fig. 8, for level flight only. In Fig. 8a, the curves show the rise in control loads with forward speed for the first series of tests where the roughness was extended in stages from the blade root, until the whole of the blade leading edge was roughened. The progressive increase in control loads with each increment of roughness displaces each curve to the left, so that the same origin can be used for all the curves in this plot.

The roughness as far as 0·4 radius makes little change to the control loads, but beyond this point, for example for the roughness applied to 0·6 radius, there is an appreciable rise in the control loads at high advance ratios. At first the advance ratio is limited to 0·3 in level flight by the engine power available, but when the roughness is extended to 0·7 radius and beyond, the requirement to keep the total amplitude of the oscillatory loading below a maximum level set for this aircraft means that the maximum permissible forward speed has to be reduced. In the worst case, when all the blade leading edge is roughened, the maximum speed has to be restricted to 60 per cent of that determined by the power limit when the blades are flown in a

smooth condition. For these test conditions (tip Mach number and thrust coefficient) this corresponds to a reduction of 45 knots indicated airspeed.

It is significant that the shape of these curves differs from the usual control load curves characteristic of the *Wessex* helicopter. Instead of the somewhat constant level of loads at moderate speeds, followed by a rather rapid rise as the limiting conditions are approached, there is an early rise in loads to a higher level than for smooth blades, which is then followed by the usual rapid rise as the limit is reached. This 'bulge' in the curves is especially apparent in the curves for roughness to 0·7 radius and 0·8 radius, and in Section 5, analysis of the control load waveform shows how it is caused by a disturbance at the front of the rotor disc initiated by the blade roughness. However, it is the subsequent steep rise at the end of the bulge which eventually leads to the limiting load. In Fig. 8b the control loads measured during tests with small bands of roughness extending only over 5 per cent of the radius in the tip region, are plotted against advance ratio. Again, only the level flight results are shown and to distinguish the various differences more easily the zero positions of the advance ratio scale are again displaced laterally. For each change of roughness location the curves are displaced 0·05 on the advance ratio scale. As in Fig. 7, the dashed curves join points of constant advance ratio, and they show how with gradually increasing speeds the radial position most sensitive to the addition of roughness moves from about 0·85 radius at $\mu = 0{\cdot}25$ to 0·95 radius at $\mu = 0{\cdot}325$. The higher advance ratio conditions are the more important, because only then do the control load levels become large, by the standard set for these experiments.

4.4. The Effect of Rate of Descent on Control Loads

In general it is found that if the helicopter is allowed to follow a descending flight path less power is required and rotor control loads are reduced. Theoretical estimates of the rotor load distribution have shown that increased control loads are usually generated by blade stall on the outer regions of the blade, and are alleviated in descending flight because the blade loading is shifted inboard as the rotor disc incidence is reduced. The measurements made to investigate the significance of this load re-distribution are shown in Fig. 9. They were made with the roughness over a small region in the tip area. Each graph denotes one of these roughness configurations, and the curves of control load against advance ratio are spaced out for clarity by displacing the zero position on the advance ratio scale as before.

The usual trend of rising control loads with forward speed is shown by each of these curves, but the effects of descent rate and location of the roughness are complicated. The discontinuities in the lifting ability of the blade caused by the leading edge roughness will interact with the complex incidence distribution induced by the vortex wake, giving rise to disturbances in control load which will vary widely in their location in azimuth. Hence the total peak-to-peak amplitude of the control load waveform which is plotted here shows a complicated dependence on advance ratio and descent rate, as the dashed lines indicate. Although these graphs present the body of the data on descent rates with tip roughness in a condensed form, it is easier to understand the significance of these parameters by extracting some of the measurements and presenting them in a slightly different way, as follows.

An appreciation of the severity of the increase in loads for each length of blade roughened can be obtained from Fig. 10a. The peak-to-peak amplitudes are plotted against the location of the 5 per cent roughness band, and the results for each descent rate arranged on a composite graph. The dotted lines show the load levels for smooth blades at each descent rate. In this form it can be clearly seen, that the roughness around 0·9 radius produces the largest increases in control loads for level flight and moderate descent rates, but the situation changes at higher descent rates, roughness around 0·8 radius producing the largest increase in loads at the highest descent rate.

In Fig. 10b curves for one of the roughness configurations have been constructed to show the level flight control loads of a range of helicopters having different values of drag. Each curve is labelled with the equivalent flat plate drag area. They are derived from Fig. 9, by choosing the appropriate rate of descent for each forward speed, according to the curves of Fig. 2. At the high speed end of the range, the curves diverge, and those corresponding to high drag values have higher oscillatory control loads. This confirms, as predicted, that the early rise in the load caused by the roughness from 0·9 to 0·95 radius, is alleviated as the loading is redistributed inboard with lower values of helicopter drag. The somewhat irregular spacing of the curves, and the different points at which they diverge, shows (on examination of the waveforms) that several mechanisms contribute to the total amplitude, only some of which are alleviated by the increasing rates of descent which correspond to the lower values of drag. It is interesting to note in Fig. 10b that the highest available advance ratio is defined by the aircraft power limit for the curves of high drag, and by the maximum rates of descent flown in these tests for those of low drag.

4.5. Interpretation of Waveforms

The control load measurements have so far been discussed only in terms of the peak-to-peak amplitude of the oscillatory load. The reasons for the growth of the oscillatory load for each roughness configuration and flight state will now be examined, using the characteristic features of the waveforms that were outlined in Section 3 and labelled types (a), (b) and (c). Examples which show the development of the waveforms with increasing forward speed and with rotor disc incidence are used to illustrate the progression of the blade stall for each roughness configuration, but it is helpful at this point to summarise the main findings before proceeding to examine the evidence in detail.

The analysis shows that the growth of oscillatory load on entirely smooth blades is due to stall in the tip region which gives rise to torsional oscillation of the retreating blade.

Roughness inboard on the blade causes blade stall at the front of the rotor disc in a region where the blade incidence is locally high due to interactions with the vortex from the preceding blade. This results in a large control load disturbance in this region of azimuth.

The waveform of the load with roughness applied in the tip region usually shows blade torsional oscillation but the azimuth position of the onset of this oscillation is found to be very dependent on the rotor disc incidence as well as the advance ratio.

Examples of the three types of waveform will now be considered in turn.

Fig. 11a shows waveforms that are typical of the smooth blade control loads. There is an oscillation at approximately six times the rotational frequency which is superimposed on the basic once per revolution variation and this oscillation is present throughout almost the whole cycle. It is assumed that this frequency of variation of the control load is associated with torsional oscillations of the blade/control system in the first mode. The trend to note from this sequence of traces is the reduction in the amplitude of this osciallation as rate of descent is increased. This type of oscillation, type (a), frequently occurs in combination with other disturbances to the blade, but it is universally true that, when present, rate of descent always reduced its amplitude, and this is primarily the mechanism for the reduction in the amplitude of the oscillatory load. It may be deduced that this disturbance is driven by the pitching moments developed on stalled areas of the blade fairly near to the tip, and the redistribution of loading accompanying a reduction in disc incidence alleviates this problem. When the oscillations grow sufficiently large to limit the speed of the aircraft, they become largest in the region of azimuth near 360 degrees, but it is interesting to note that the oscillations are continuous after about 140 degrees.

The addition of roughness inboard on the blade brings into play the disturbance type (b) at the front of the rotor disc. This special feature which is associated with the vortex crossing position, is shown in the example in Fig. 11b. The first three waveforms at the top of the page show the gradual onset of this disturbance as forward speed is increased in level flight for the condition where the blade leading edge is roughened from the blade root to 0·6 radius. Forward speed is further increased in the lower two waveforms, but for these cases rate of descent is required, first to avoid the level flight power limit and then for the highest speed, to keep the total peak-to-peak amplitude below the maximum by suppressing the retreating blade oscillation. Note however, that in this case the disturbance at the front of the disc continues to grow as speed is increased.

Fig. 11c shows the onset of this disturbance (type (b)) in level flight for the blade roughened to 0·7 radius. The 'spike' in the curve appears at a lower value of μ than for the blade roughened to 0·6 radius, and comparisons made at the same advance ratios (e.g. $\mu = 0{\cdot}27$ and again at $\mu = 0{\cdot}28$) show that for a given forward speed the disturbance is now much larger. In Fig. 11d the effects of rate of descent and rotor thrust coefficient for this extent of roughness are shown. The first two curves at the top of the page show the earlier onset of the disturbance in level flight compared with the lower thrust coefficient examples in Fig. 11c. The following two curves in Fig. 11d then illustrate how with increasing rate of descent, the disturbance at the front of the disc is increased in amplitude. This trend is typical of many of the flight conditions tested, and may be attributed to the redistribution of loading along the blade, local incidences becoming less near the tip and greater inboard, as the descent rate is increased.

The conditions which give rise to this disturbance at the front of the rotor disc in level flight are summarised in Fig. 12. Curves are plotted from the measured data to show the roughness extent and forward speed combinations which coincide with the onset of this disturbance in the control load waveform. Values of the rotor thrust coefficient and rotational tip Mach number are constant for each curve. The disturbance becomes increasingly large in areas of the graph to the right of each boundary.

As the waveform examples have shown, these boundaries in Fig. 12 confirm that increasing forward speed eventually gives rise to this disturbance, and that the speed at which it is first apparent is reduced as the

roughness is gradually extended from the blade root. As anticipated, the higher mean blade loadings at a high thrust coefficient give rise to an earlier onset of the disturbance, and for regions towards the blade tip, the sensitivity of the aerofoil performance to Mach number is revealed by the separation of the boundaries beyond 0·7 radius.

The shape of each of these boundaries also reveals something of the loading along the blade at this azimuth position (compare Fig. 5a). The incidence distribution depends on the trim of the whole rotor, which in turn will depend on the performance limitations of the blade at other azimuth positions, but it seems certain that there is a region near the root where the addition of roughness will produce little change in the boundaries. Similarly, near the blade tip, if the general incidence level is well below the stall, further extension of the roughened region will produce no change in the value of μ for the onset of the disturbance. Hence the vertical trend of the boundaries in these two regions.

The most interesting part of these boundaries is the central region, where the progressive increase in the radial extent of the leading edge roughness begins to reduce the speed for the onset of the disturbance. The straight line drawn diagonally across Fig. 12 defines the radial location of the tip vortex from the previous blade (making the same undistorted wake assumptions as for the construction of Fig. 6). Roughening the blade has little effect on the onset of this disturbance until the portion of the blade above this line, which is influenced by the upwash from this trailing vortex, is roughened.

Both the changes in the mean inflow and the local flow perturbations in this region due to the displacement effect of the fuselage, will cause an increasing share of the load to be taken inboard on the blade as speed is increased, contributing to the trends shown by these boundaries. However, the position of the onset, and the rapid growth of this disturbance to quite a large amplitude indicates that it is the roughness, causing the blade to stall in the highly loaded region affected by the vortex upwash, which is the primary cause of this disturbance, rather than a more gradual extension of an inboard stalled area out along the blade. If a change of pitching moment coefficient with stall of 0·15 is assumed, this would require approximately four chord lengths of the blade to be stalled in the localised region of upwash, which is consistent with the interpretation of events described. Note that the dashed portion of the curve (Fig. 12) for the lowest Mach number is for a measurement in descending flight. The oscillatory behaviour of the retreating blade dominates the waveform shape at these advance ratios and it is only the suppression of this oscillation by rate of descent, that allows the presence of the disturbance at the front of the disc to be detected. It is a very weak disturbance as the vortex has moved far inboard at this speed, and at higher advance ratios it is expected to disappear altogether.

Examples of the third main feature of the control load waveform, type (c), described in Section 3, are presented in Fig. 13a and b. This is the large upward-going excursion in the load which appears just before zero azimuth position. Fig, 13a illustrates the onset and growth of this disturbance, and Fig. 13b the way in which, like all the disturbances which are attributable to regions of the blade towards the tip, it is alleviated by increasing rate of descent as more of the load is taken inboard. This disturbance contributes substantially to the total oscillatory amplitude because it adds to the basic first harmonic (once per revolution) variation in control load. For the Wessex helicopter the first harmonic has a peak nose-down excursion in the azimuth region of 180 degrees, which contributes to the local disturbance at 180 degrees, and similarly at azimuth zero, the peak nose-up excursion of the first harmonic adds to this brief oscillatory disturbance. For rotors where the concern is a fairly large first harmonic variation of pitching moment due to blade camber, the phasing of these disturbances might appear to be less significant.

The examples in Fig. 11a to d and Fig. 13a and b were chosen to isolate the special features identified, but amongst the many combinations of these features that were recorded, certain cases are of special interest, and are shown in Fig. 14. The curve (a) shows how, provided the thrust coefficient is high enough, the disturbances at the front and back of the rotor disc appear even at a very small advance ratio. This example also demonstrates that roughness over most, or all, of the blade brings into play these two disturbances, in contrast to the behaviour of the smooth blade, where even at high thrust coefficients the retreating blade oscillation dominates the waveform. Example (*b*) shows the retreating blade oscillation at high advance ratio. This waveform shape is characteristic of the moderately high advance ratios in level flight, and the highest advance ratios in descents, both for the completely smooth blades and those roughened in the 0·8 radius region. Note that the torsional oscillations vary in amplitude but persist round the whole cycle. This can occur at low advance ratios also, for high thrust coefficients. Fig. 14c shows a trace recorded in hovering flight. The shape is dominated by the loads associated with torsional oscillation of the blade. Pressures recorded during this flight condition show that at 0·92 radius the blade is periodically stalling as it interacts with the tip vortices of preceding blades. In conditions where the tip vortices are visible due to condensation in the vortex cores it can be observed (and some ciné film records have been made) that the vortices weave

around close to the track of the blades, some apparently passing above the following blade. Only the flights where the extreme tip regions of the blades, between 0·95 and 0·98 radius, were roughened produced this stall flutter type of oscillation. All the other configurations failed to produce these oscillations even at thrust coefficients up to the power limit of the aircraft.

4.6. Complementary Measurements

The signature of the blade pitch link load reflects the consequences of limiting the lifting ability of each portion of the blade and has been used as described in the previous sections to deduce which parts of the blade are induced to stall. During the tests detailed surface pressure measurements were recorded on the other pair of modified blades, together with certain blade bending strains and a single 'stall indicator' pressure sensor[1] output from one of the roughened blades.

The blade bending strain measurements confirmed that no exceptionally high stress levels were caused as a result of the modifications to the rotor blades, or by operating beyond the normal flight limits, but they did reveal that certain blade bending modes were excited to a higher amplitude in descending flight than in the corresponding level flight conditions. The 'stall indicator' pressure sensor fitted to one of the roughened blades helped to confirm which regions of the blade were stalled at each azimuth position. The stall and stall recovery cycles which followed the blade torsional oscillations could be clearly identified, and the output confirmed that in extreme cases where roughness is applied near the blade tip, the blade remained stalled at 0·91 radius for almost one third of a revolution.

Fig. 15 presents sample results from the pressure-measuring test section flown on the modified blades of this helicopter. They were copied directly from a visual display unit. The upper 'curve' represents an upper surface pressure measured at a chordwise position of 0·025 chord, for the test section at 0·92 radius and an advance ratio of 0·39. Samples (each point on the plot) are taken at one degree intervals of azimuth position. The large and rapid variations of pressure which are caused by the wake interactions and subsequent stalling of the blade at this radius are well demonstrated in this example. The lower three graphs in Fig. 15 show the corresponding force and moment coefficient variations during one turn of the rotor. The normal force (C_N) illustrates the very sudden lift changes which occur, and the chordwise force (C_T) plot reveals very clearly the associated changes in the leading edge suction peak. The bottom graph (C_M) shows the variation in section pitching moment coefficient. The general unsteadiness and rapid fluctuations in the region of 270 degrees azimuth position give an appreciation of the way in which the pitching moments and corresponding control loads are generated.

Although only samples of the pressure measurements are presented here, they were recorded for all the flight conditions tested. The stress measurements are important, not only from airworthiness considerations, but because the motions which result from the excitation of the various blade bending and torsional modes directly affect the aerodynamic loads via the incidence changes they produce. The pressure measurements help to confirm, at least qualitatively, that the theoretical models used in interpreting dependence of the control loads on blade leading edge roughness, are correct.

5. Discussion

A total of ten different roughness configurations have been tested (Fig. 1). From the seventeen sorties flown, each of approximately one hour's duration, a sufficient body of control load data has been recorded to enable the lift requirements of various parts of the blade to be determined. The results can be used to give an indication of the possibility of raising rotor performance limits and minimising control loads by using reflex camber inboard and relatively high positive camber in the tip region. The wide range of thrust coefficient, Mach number and rotor disc incidence investigated, together with an interpretation of control load disturbances in terms of uniform flow and blade tip vortex interaction, provide the means for estimating limits for other rotors too.

The results from the first part of these experiments, which explore the possibility of applying reflex camber inboard on the blade, have shown that a disturbance not normally present on this helicopter with smooth blades is initiated at the front of the rotor disc when the maximum lift coefficient is reduced by leading edge roughness (Fig. 11b, c and d). The way in which the onset of this disturbance is related to the rotor wake is shown in Fig. 12, and the magnitude can be judged from the curves of Fig. 8a. Close examination of the waveforms from which these curves were obtained reveals that in general, the disturbance associated with this particular wake crossing does not initiate a growing torsional oscillation, but one that is largely damped out after the initial nose-down excursion. Although this excursion can be large enough to bring the overall amplitude up to the limit for this aircraft, the fact that in this azimuth region, a disturbance can be damped

after a single excursion, reduces the probability that this type of disturbance will generate very high control loads. (A stronger control system may be quite capable of sustaining the load levels generated.) Thus, roughness can be extended to 0·6 radius without significantly reducing the maximum permissible speed of this helicopter, and it is not until the roughness extends to 0·7 radius that the rapid rise of control loads, associated with the onset of the retreating blade oscillations, begins to reduce the permissible maximum speed in level flight.

In assessing the relevance of this particular disturbance to helicopters other than the *Wessex*, the displacement of the flow by the fuselage must be considered. Blade incidences are raised in this region of the rotor disc by an increment proportional to the advance ratio because of the upward deflection of the flow above the nose of the fuselage, reducing the threshold for the onset of blade stall. The tip vortex from the previous blade will be displaced slightly towards the rotor disc but this will only give rise to very localised changes in the blade incidence distribution. Although the fuselage of the *Wessex* is a rather bluff shape of relatively large maximum cross section, its small extension forwards of the shaft reduces flow deflections near the plane of the disc, except near the rotor hub. The installation of engines aft of the rotor shaft in more recent designs necessarily requires a relatively larger extension of the fuselage towards the front of the rotor disc for trim. Calculations show that for such layouts the upwash will be increased at the front of the rotor disc, and the mean incidence levels will be raised compared with those of the present tests.

The design of a rotor to employ reflex camber in this way must depend on many factors, for example, the particular type of reflex section chosen, and the amount of blade twist, but it seems clear from these results that the blade may be given reflex camber out to 0·6 or 0·7 radius without any significant rise in the control loads. This radial extent is quite sufficient to permit substantial cancellation of the pitching moments that would be generated by cambered blade tips on the advancing side of the rotor.

The second part of the experimental programme was concerned with the application of roughness to small lengths of the blade in the tip region. The increased control loads give a measure of the lift demands on each part of the blade so treated. The special feature of the control load waveforms associated with roughness in the extreme tip region is the sudden increase of the torsional oscillation to a large amplitude around the rear of the rotor disc, Fig. 13a. More generally, an earlier onset of the retreating blade torsional oscillation was the result of roughness bands between 0·85 and 0·95 radius. With the creation of a discontinuity of maximum lift coefficient along the blade, the sudden rise in loads characteristic of the completely smooth blade is replaced by a more gradual rise with increasing speeds.

The speed at which the control loads become large enough to limit the speed of the helicopter, or the absolute magnitude of the loads at any lower speed, is not particularly important for these roughness bands in the tip region. The discontinuities created by the roughness are bound to create patterns of separation which are not representative of those on any optimised rotor where the lifting ability is tailored to the demands. The value of these measurements lies in comparing the relative control load levels at various advance ratios in Fig. 8b, Fig. 9 and Fig. 10. The sections of blade most sensitive to the application of roughness would then be expected to show the greatest performance improvement for an improvement in section performance, for that particular advance ratio and helicopter drag. Although the substance of these results is of a qualitative nature, it is interesting to note that the magnitude of the increase in control load levels with the 5 per cent radius roughness bands is comparable with the rise attributable to the increase in Mach number of 7·5 per cent with unroughened blades (Fig. 7a and b).

6. Conclusions

Surface roughness has been applied systematically to portions of the leading edge of a *Wessex* helicopter blade to reduce the local value of maximum lift coefficient. The extent to which the inner portions of the blade could sustain reduced maximum lift coefficient without reaching limiting control loads has been investigated.

In a similar way, but using local bands of roughness in the tip region, those areas of the blade which stall first and are therefore likely to provide the largest potential gain from an improved lifting capability have been identified.

The technique of systematically varying the rotor performance parameters for each roughness configuration has provided a large body of measurements of control load waveform. The various signatures contribute to the general understanding of the limitations associated with each part of the rotor blade, while helping to achieve the specific objectives discussed above.

All the roughness configurations tested produced increased control loads for all the flight conditions flown. At low speeds (except in hovering flight) the differences were small, but as speeds were increased, there was

an earlier rise in the oscillatory loads for the roughened blades. Increases in rotor thrust coefficient or Mach number produced higher loads, as was the case for the smooth blades. Descending flight paths, flown to represent the lower disc incidence associated with helicopters having a lower drag, alleviated the control loads for smooth blades, and for any roughness configuration flown during which stall occurred first in the tip region.

The measurements suggest that if profiles with reflex camber, resulting in this instance in a reduction in $C_{L\,max}$ of 0·2, were used on the inner portion of the *Wessex* blade to offset pitching moments from high lift sections nearer the tip, their use beyond 0·4 radius would lead to the premature onset of control load disturbance at the front of the rotor disc. If used beyond 0·6 radius, the effect of this disturbance would be large enough to necessitate a limit on speed of the *Wessex* helicopter. By revealing the nature of this disturbance these results provide a means of estimating the significance of this limitation for future designs where sections with increased maximum lift coefficient and pitching moment could be used to advantage in the tip region but in combination with different control system strength, fuselage layout, number of blades and twist distribution.

In investigating the tip region of the rotor blade, the onset of the retreating blade oscillations, which eventually generate the limiting control loads, has been found to be particularly dependent on the performance of the blade profile between 0·8 and 0·9 radius. Reductions of maximum lift coefficient even nearer to the blade tip create large control load disturbances at the rear of the rotor disc. However, in general terms, sensitivity at each radial position is very dependent on blade-wake interaction which varies with advance ratio, and also with overall radial load distribution governed by rotor disc incidence.

LIST OF SYMBOLS

A	drag area
A_w	drag area for *Wessex*
b	number of blades
c	blade chord
C_N	normal force coefficient
C_T	chordwise force coefficient
C_M	pitching moment coefficient
$C_{L\,\max}$	maximum lift coefficient
D	drag
L	lift
$M_{T\,\mathrm{rot}}$	rotational tip Mach number
r	radial position on blade
R	blade radius
t_c	rotor thrust coefficient = $T/\rho bcR(\Omega R)^2$
T	thrust
V	velocity along flight path
W	weight
x	chordwise station
α_D	rotor disc incidence
μ	advance ratio
ρ	air density
σ	density ratio
ϕ	flight path angle
ψ	azimuth angle
Ω	rotor speed
ω	rotor speed ratio = rev/min/220

REFERENCES

No.	*Author(s)*	*Title, etc.*
1	P. Brotherhood and D. W. Brown ...	Flight measurements of the effects of simulated leading edge erosion on helicopter blade stall, torsional loads and performance. A.R.C. R. & M. 3809 (1977)
2	M. J. Riley and P. Brotherhood	Comparative performance measurements of two helicopter blade profiles in hovering flight. A.R.C. R. & M. 3792 (1977)
3	E. A. Beno	Analysis of helicopter manoeuvre-loads and rotor-loads flight test data. N.A.S.A. CR-2225 (1973)
4	J. Scheiman	A tabulation of helicopter rotor-blade differential pressures, stresses, and motions as measured in flight. N.A.S.A. TM X-952 (1964)

APPENDIX

The Use of Descending Flight to Simulate Lower Values of Helicopter Drag

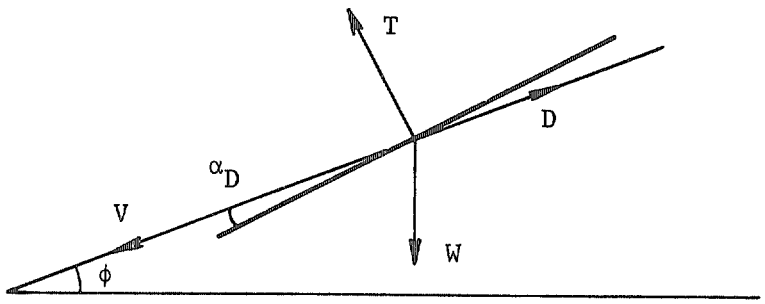

Rotor loads measured in descending flight can be used to predict the loading action in level flight associated with a similar helicopter having a reduced drag.

For small angles of descent

$$T = W, \qquad D = T\alpha_D + W\phi \quad \text{and} \quad D = \tfrac{1}{2}\rho V^2 A_w,$$

where A_w is the 'drag area' or equivalent flat plate area of the *Wessex* helicopter, and the rotor in-plane force is included in the drag force, D, or

$$\frac{\tfrac{1}{2}\rho V^2 A_w}{W} = \alpha_D + \phi.$$

If A is the drag area that would give this disc incidence in level flight, then

$$\frac{\tfrac{1}{2}\rho V^2 A}{W} = \alpha_D$$

so the flight path angle for each drag area is given by

$$\phi = \frac{\tfrac{1}{2}\rho V^2}{W}(A_w - A)$$

Values of disc incidence and rate of descent for a range of true airspeeds are shown in Fig. 3. The value of 3·34 m^2 for A_w is derived from trim measurements made on this aircraft and an average test weight is taken as 4850 kg. Drag areas of 2·9 m^2, 1·2 m^2 and 0·835 m^2 have been chosen to represent lower drag values of interest. These drag areas correspond to values of L/D_{100} of 25, 40, 70 and 100 respectively, where D_{100} is the drag at 100 ft/s (see Fig. 10b).

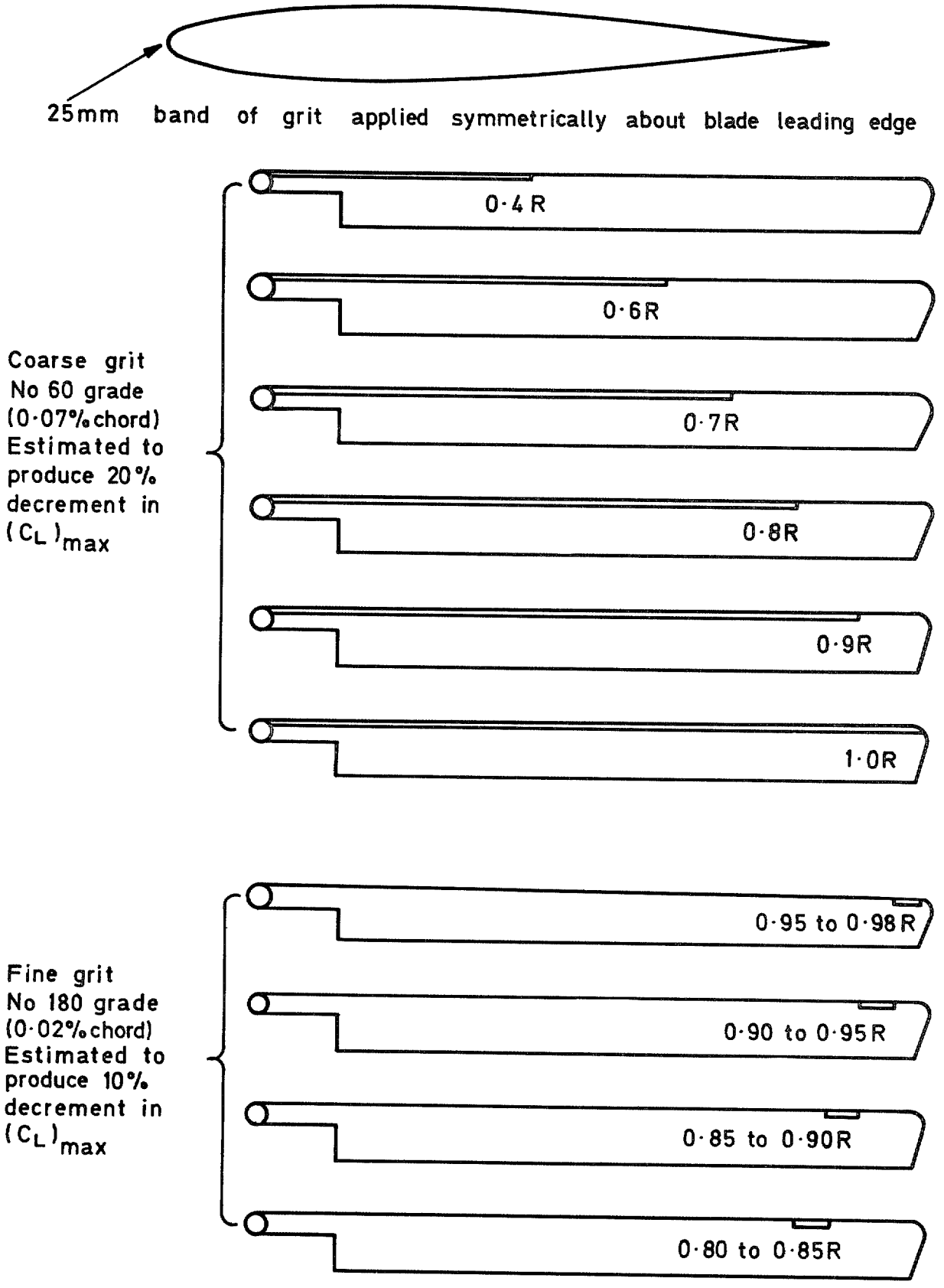

FIG. 1. Leading edge roughness configurations.

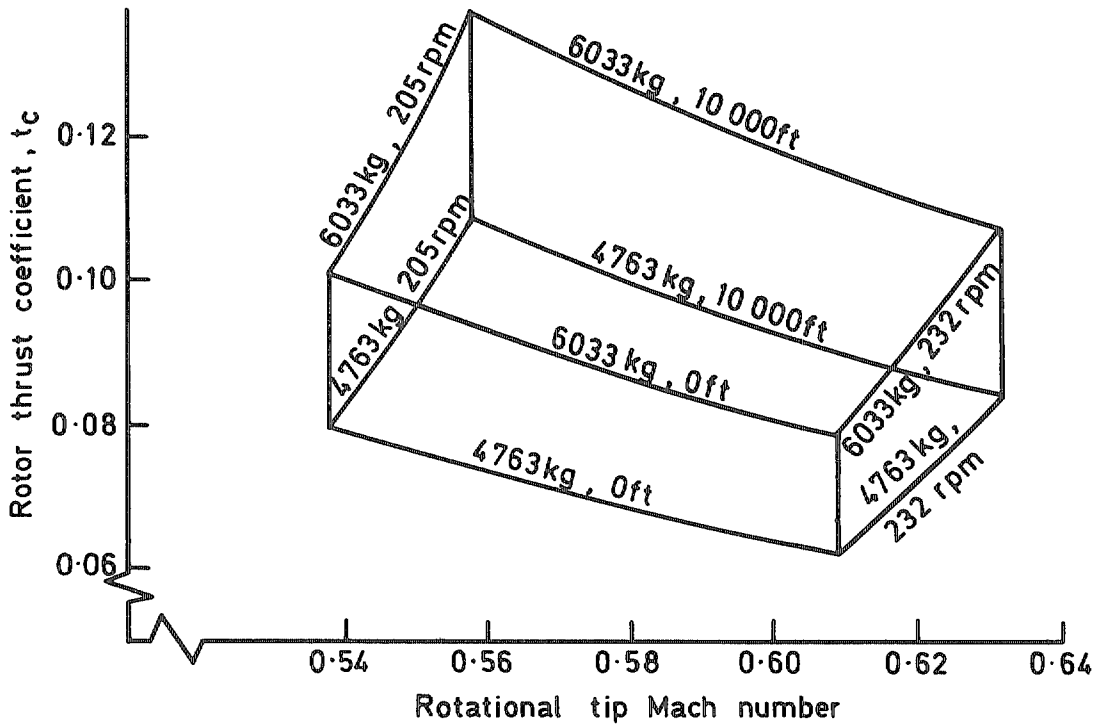

FIG. 2a. Extended Mach number and thrust coefficient boundaries for *Wessex*.

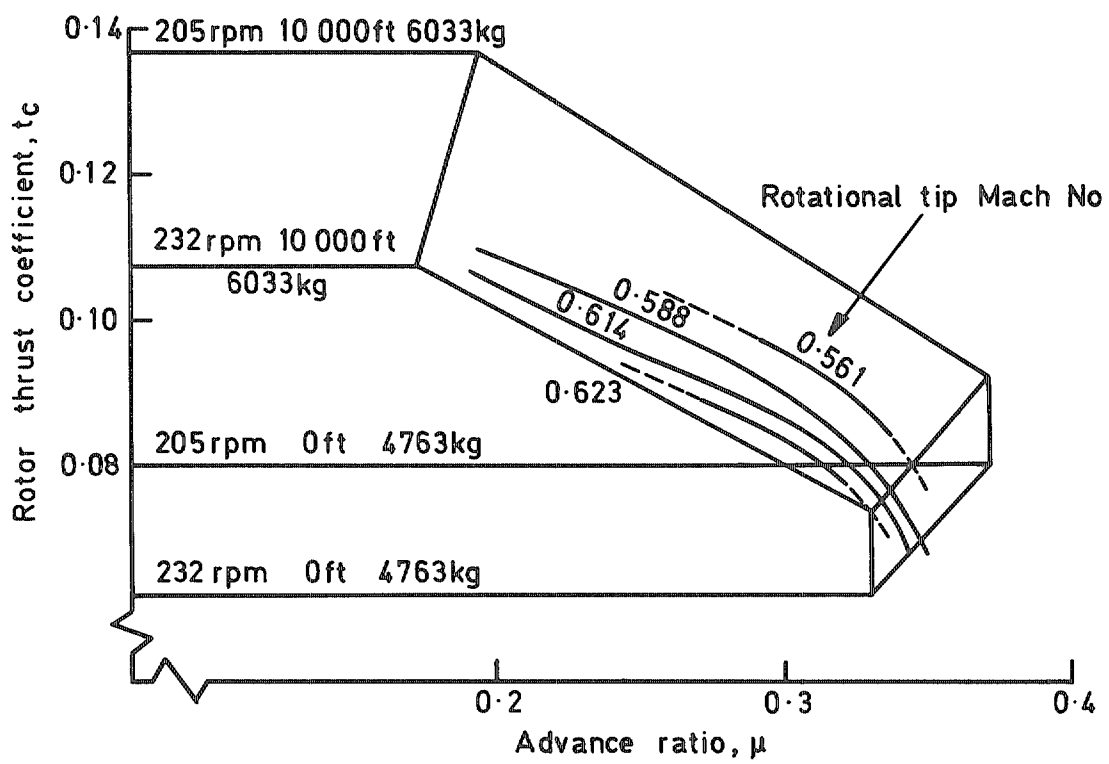

FIG. 2b. Permitted advance ratio and thrust coefficient boundaries with measured control load limits for unroughened blades shown superimposed.

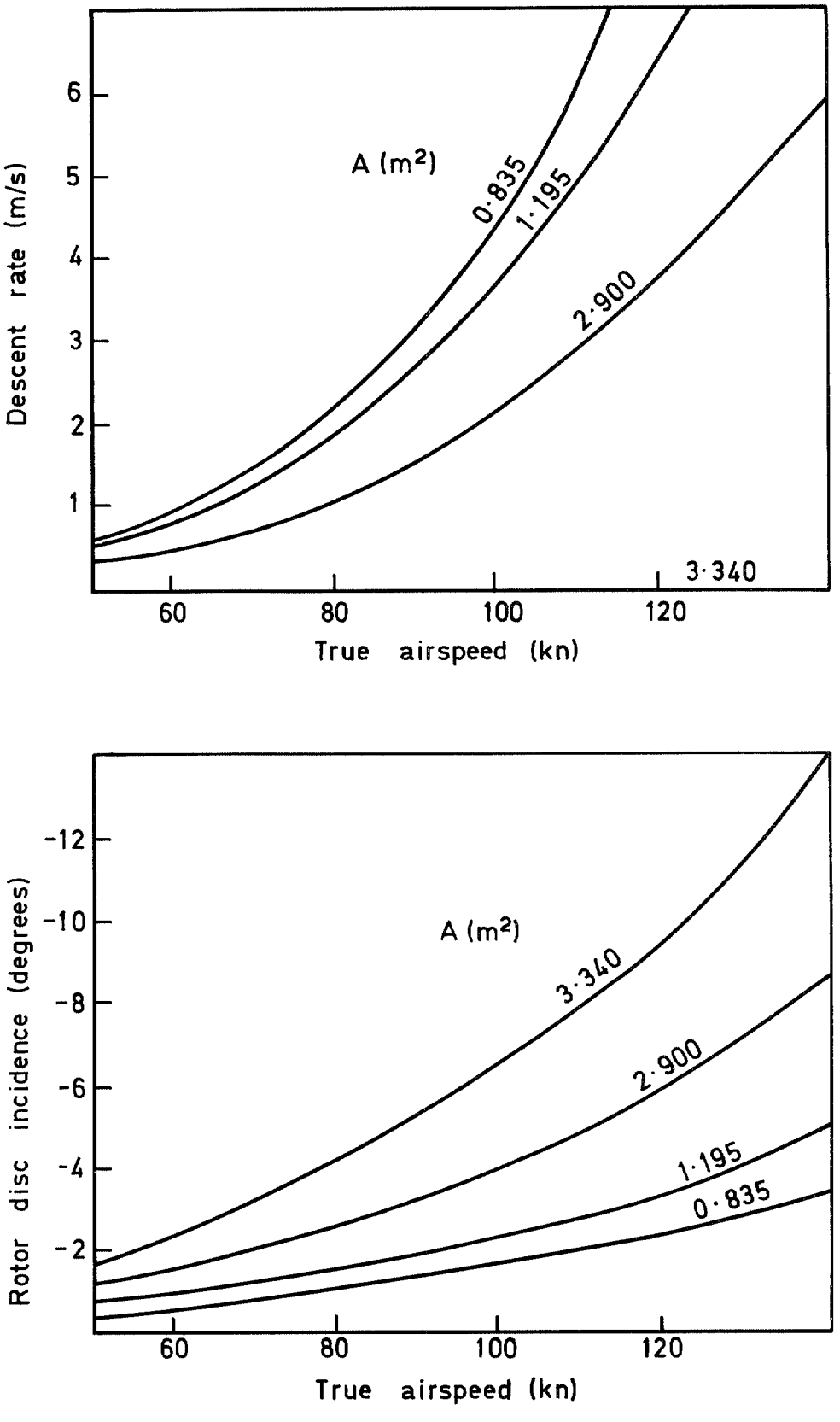

FIG. 3. Rate of descent necessary to give rotor disc incidence corresponding to reduced helicopter drag.

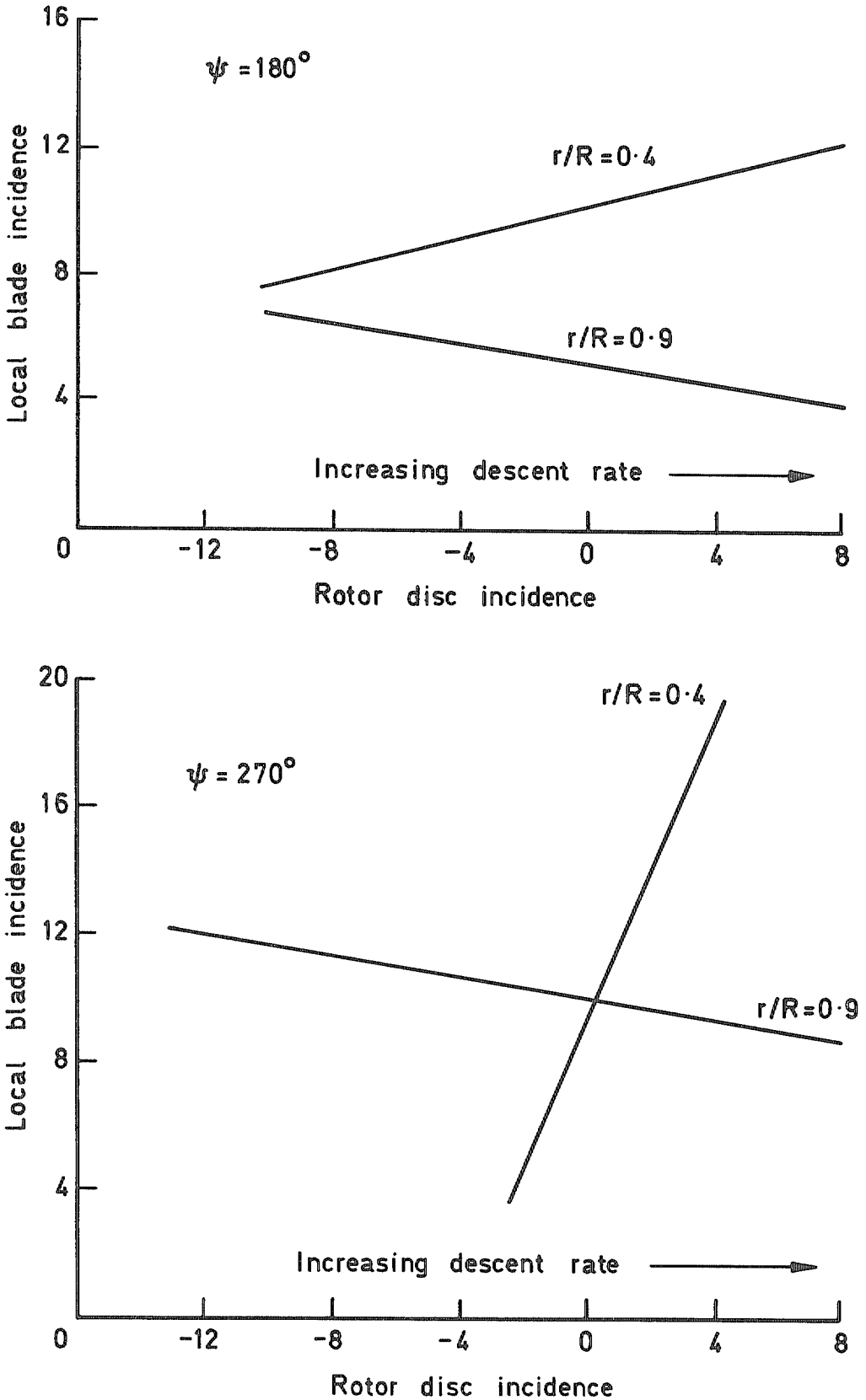

FIG. 4. The re-distribution of blade loading towards the blade root as rate of descent is increased, at $\psi = 180°$ and at $\psi = 270°$.

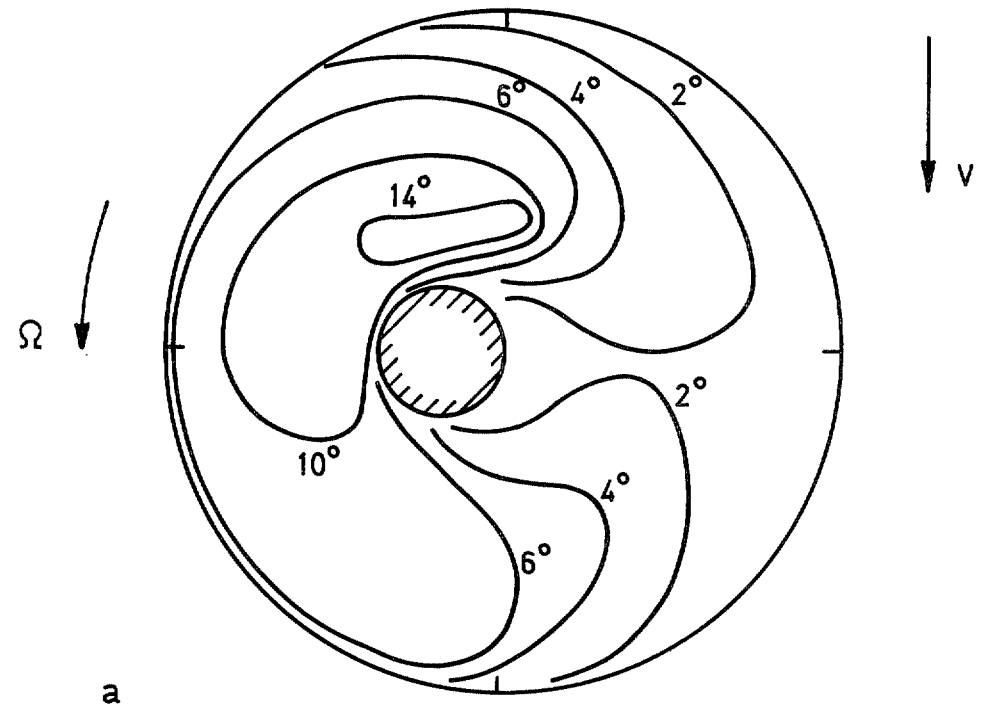

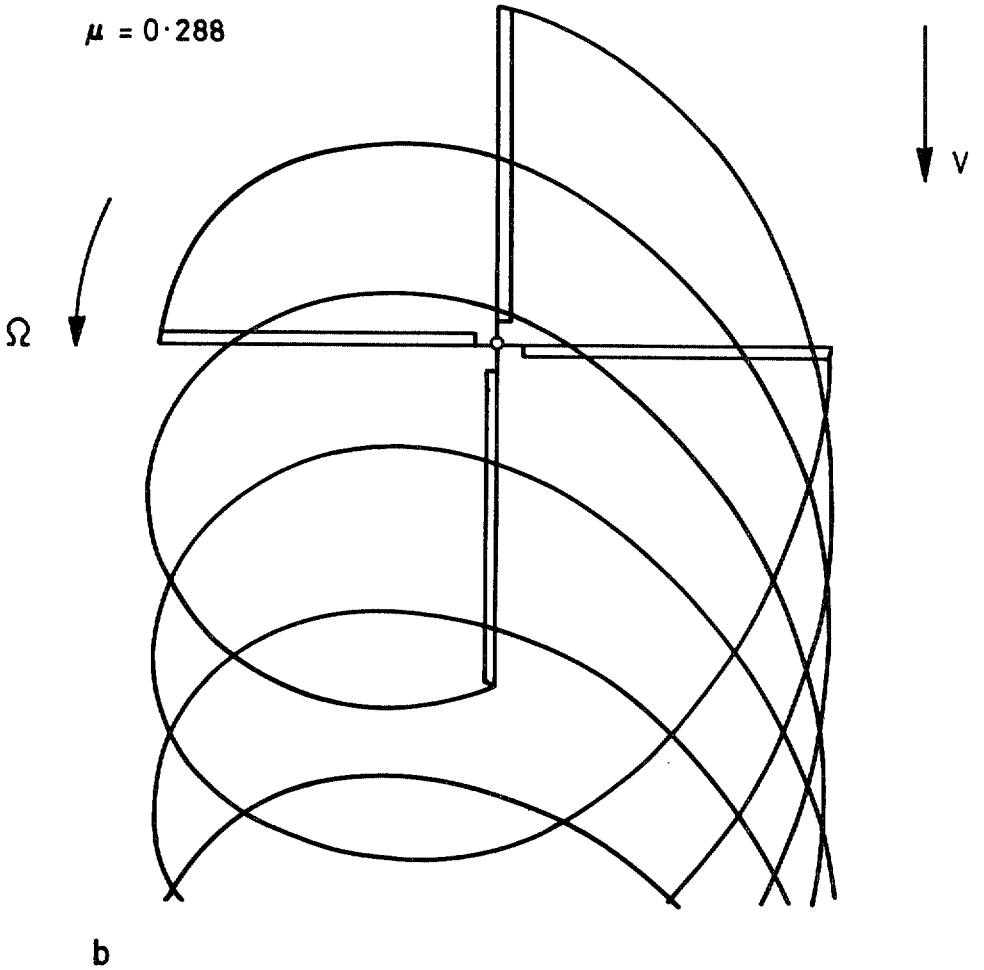

FIG. 5a & b. Measured incidence contours from Ref. 4, a and corresponding tip vortex positions, b.

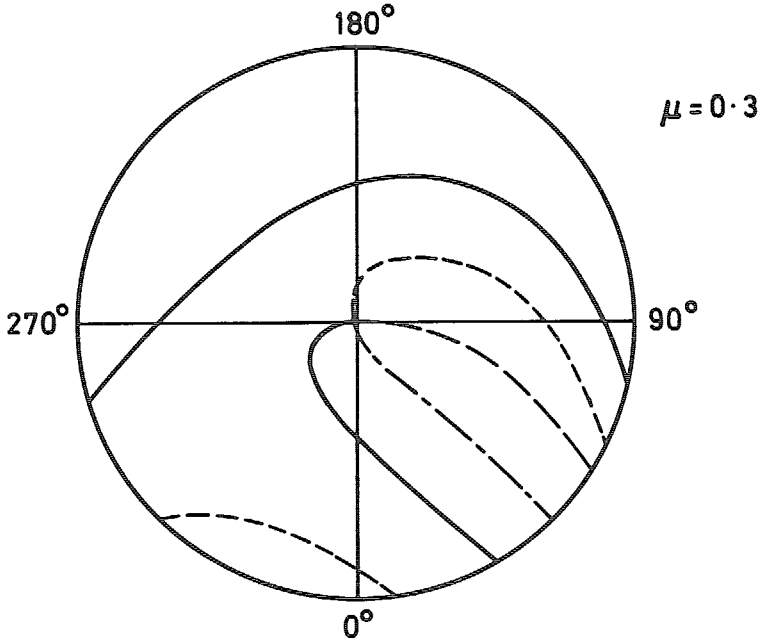

Previous blade

Opposite blade

Following blade

Same blade

a

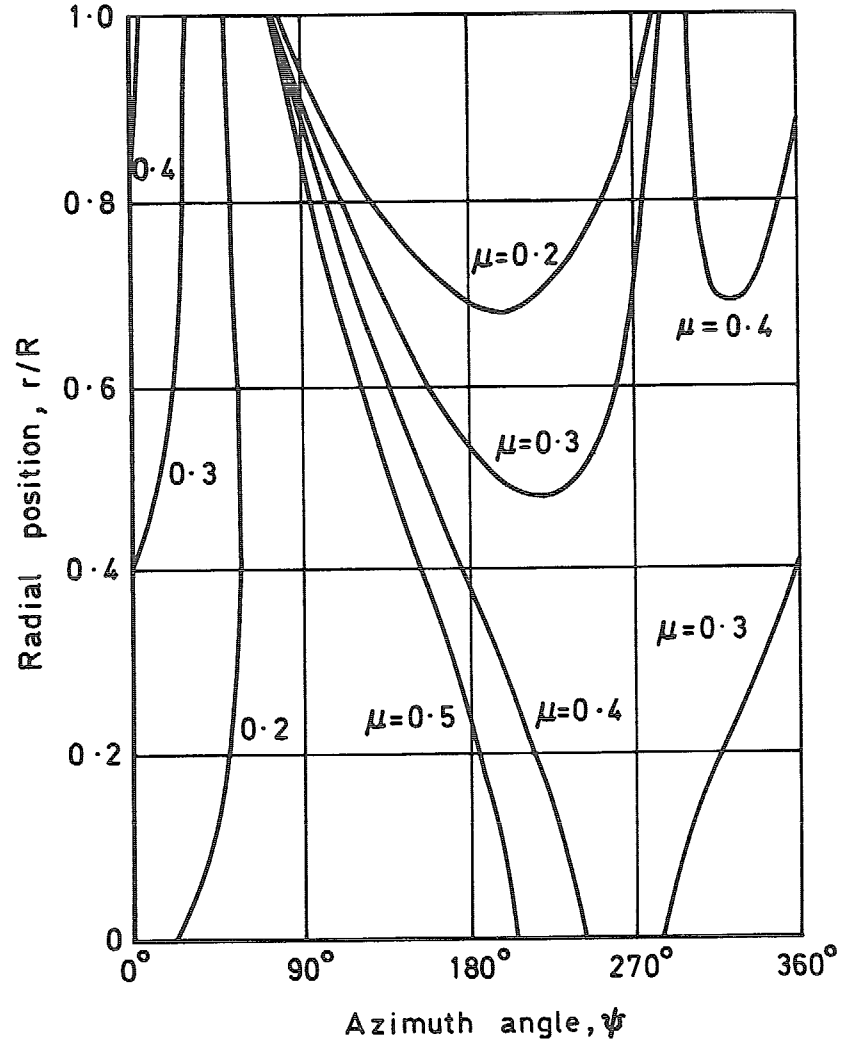

b

FIG. 6a & b. Blade-vortex crossing points derived from cycloidal wake model.

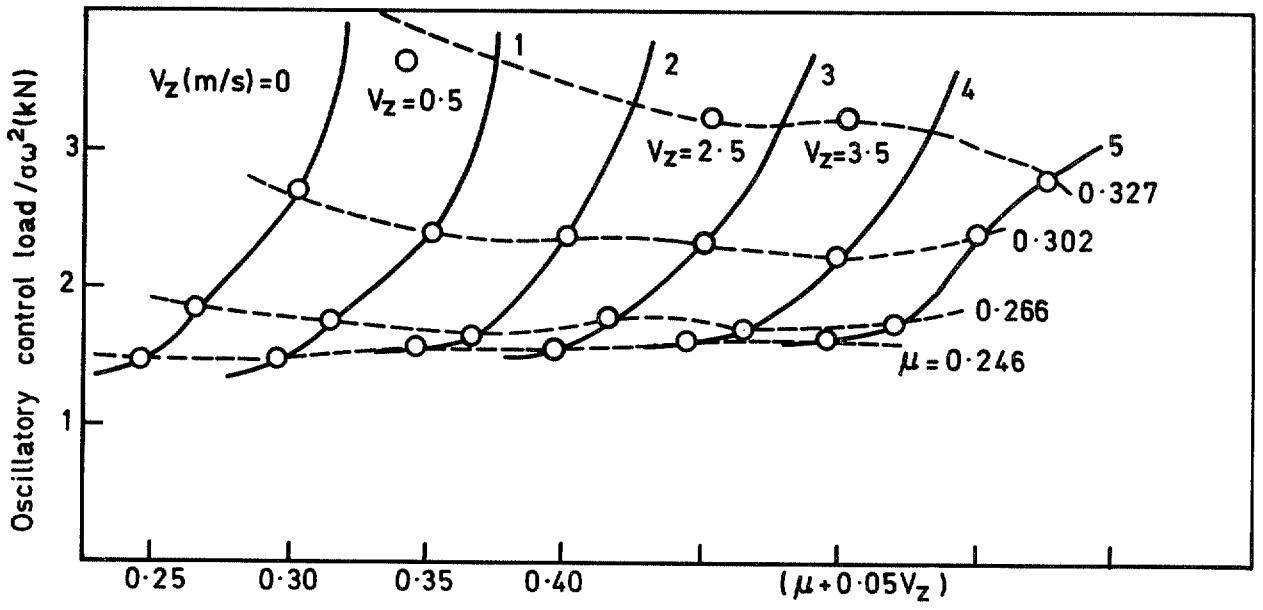

FIG. 7a. Peak-to-peak amplitudes of oscillatory control loads for unroughened blades $(M_T)_{rot} = 0{\cdot}588$, $t_c = 0{\cdot}0853$.

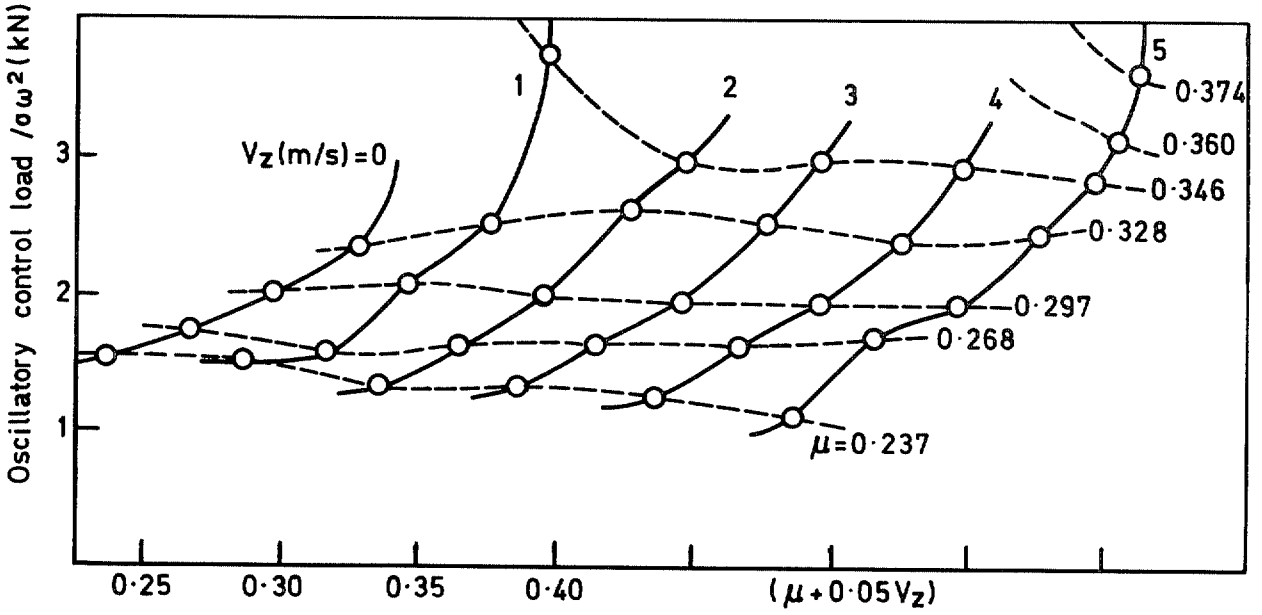

FIG. 7b. Peak-to-peak amplitudes of oscillatory control loads for unroughened blades $(M_T)_{rot} = 0{\cdot}547$, $t_c = 0{\cdot}0853$.

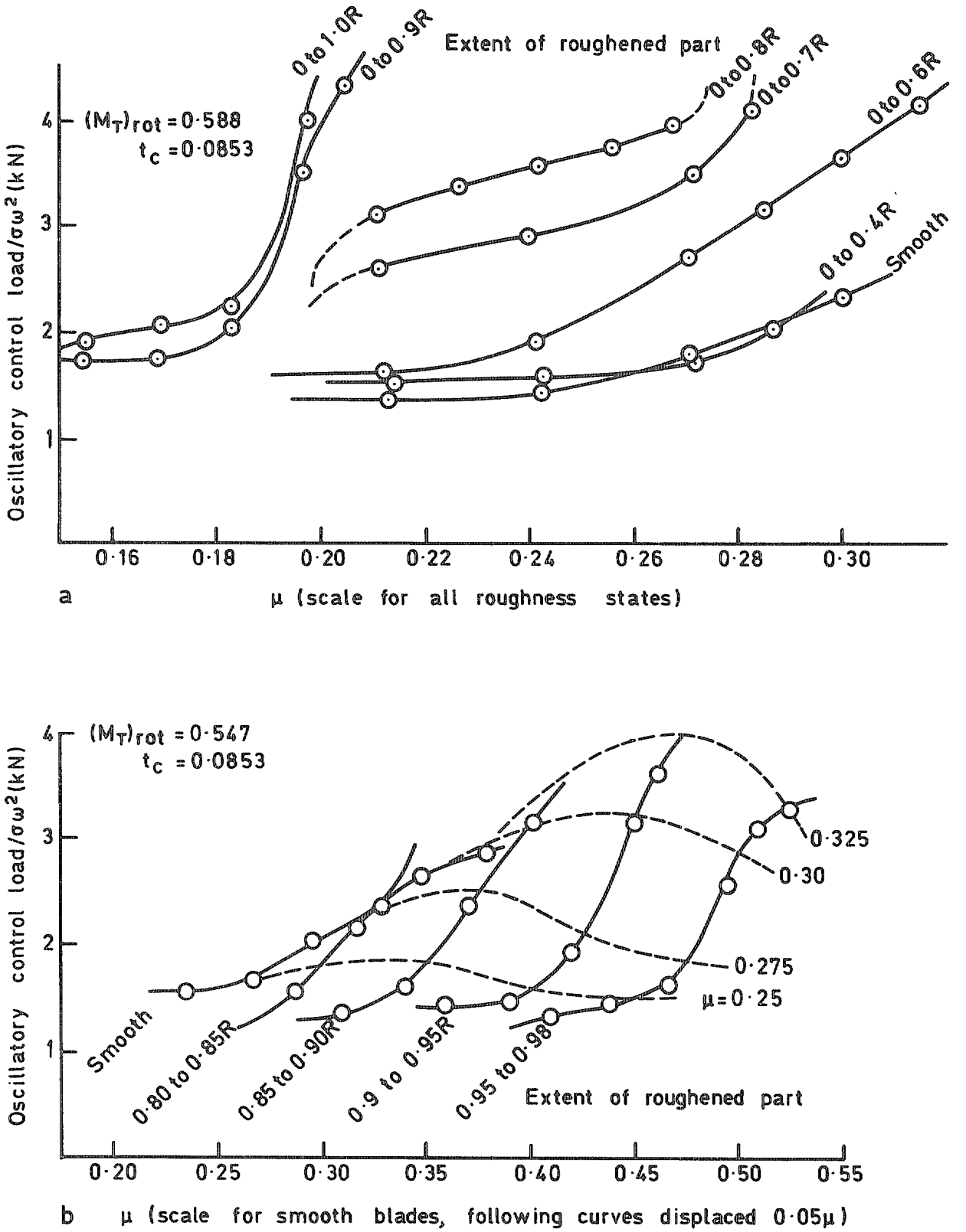

FIG. 8a & b. Peak-to-peak amplitude of oscillatory control loads in level flight.

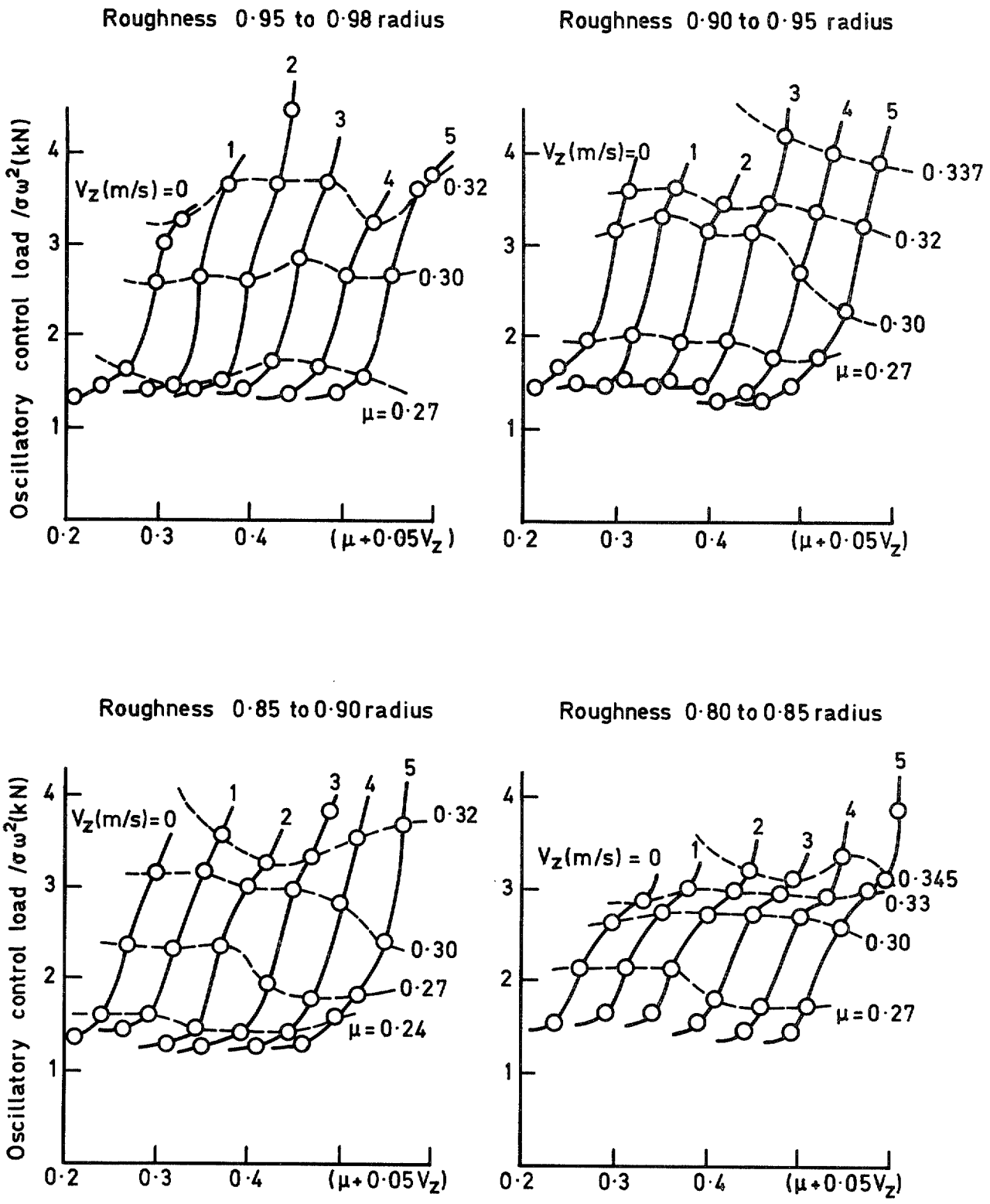

FIG. 9. Peak-to-peak amplitude of oscillatory control load in descending flight for the 5 per cent roughness bands in the tip region.

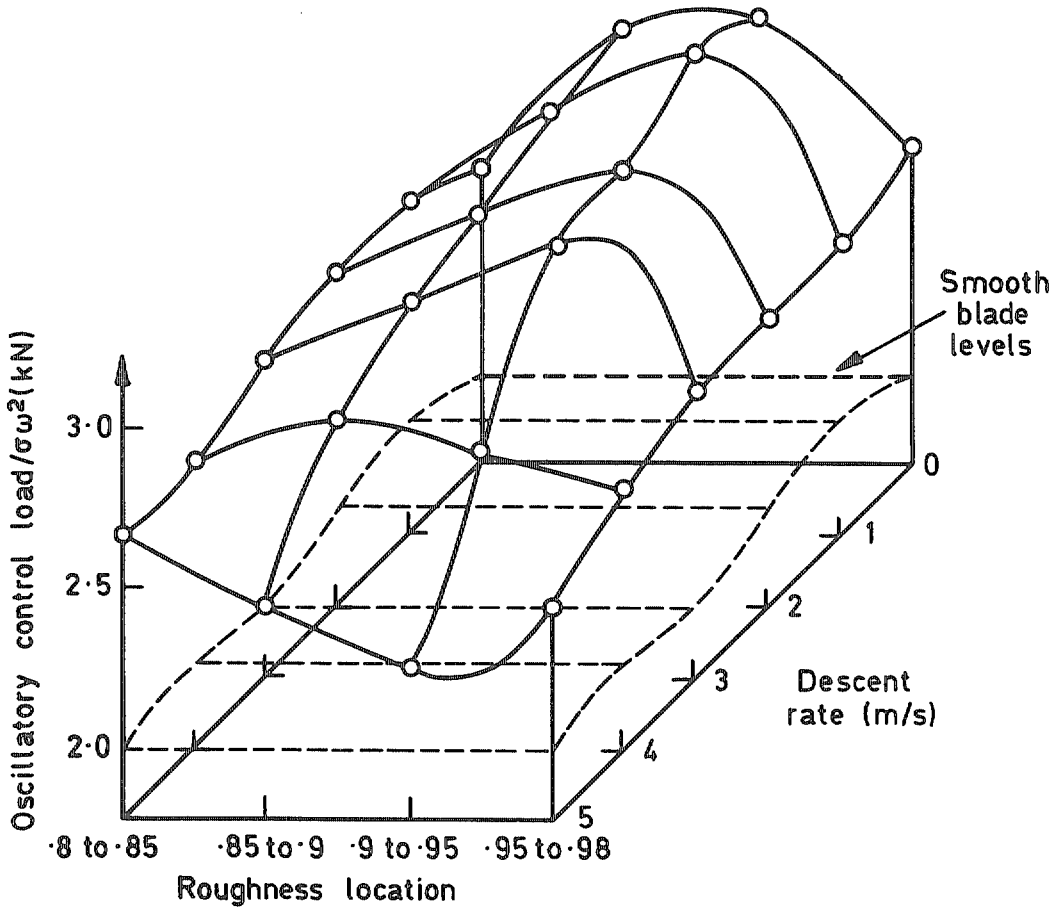

FIG. 10a. Variation of control load with roughness location for a range of descent rates at $\mu = 0{\cdot}3$.

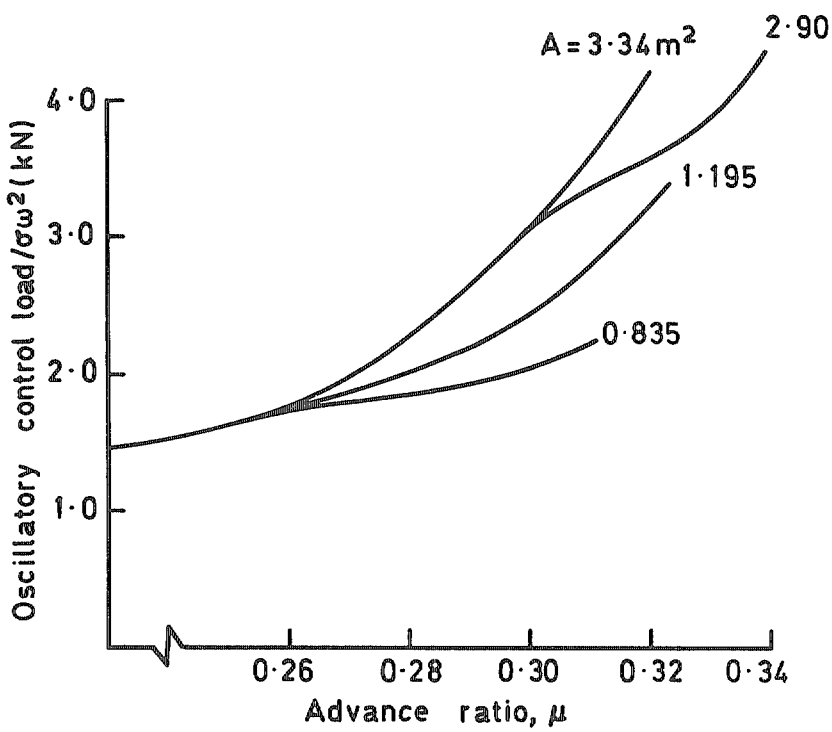

FIG. 10b. Control loads for different helicopter 'drag areas' with roughness from 0·9 to 0·95 radius. $(M_T)_{rot} = 0{\cdot}547$, $t_c = 0{\cdot}0853$.

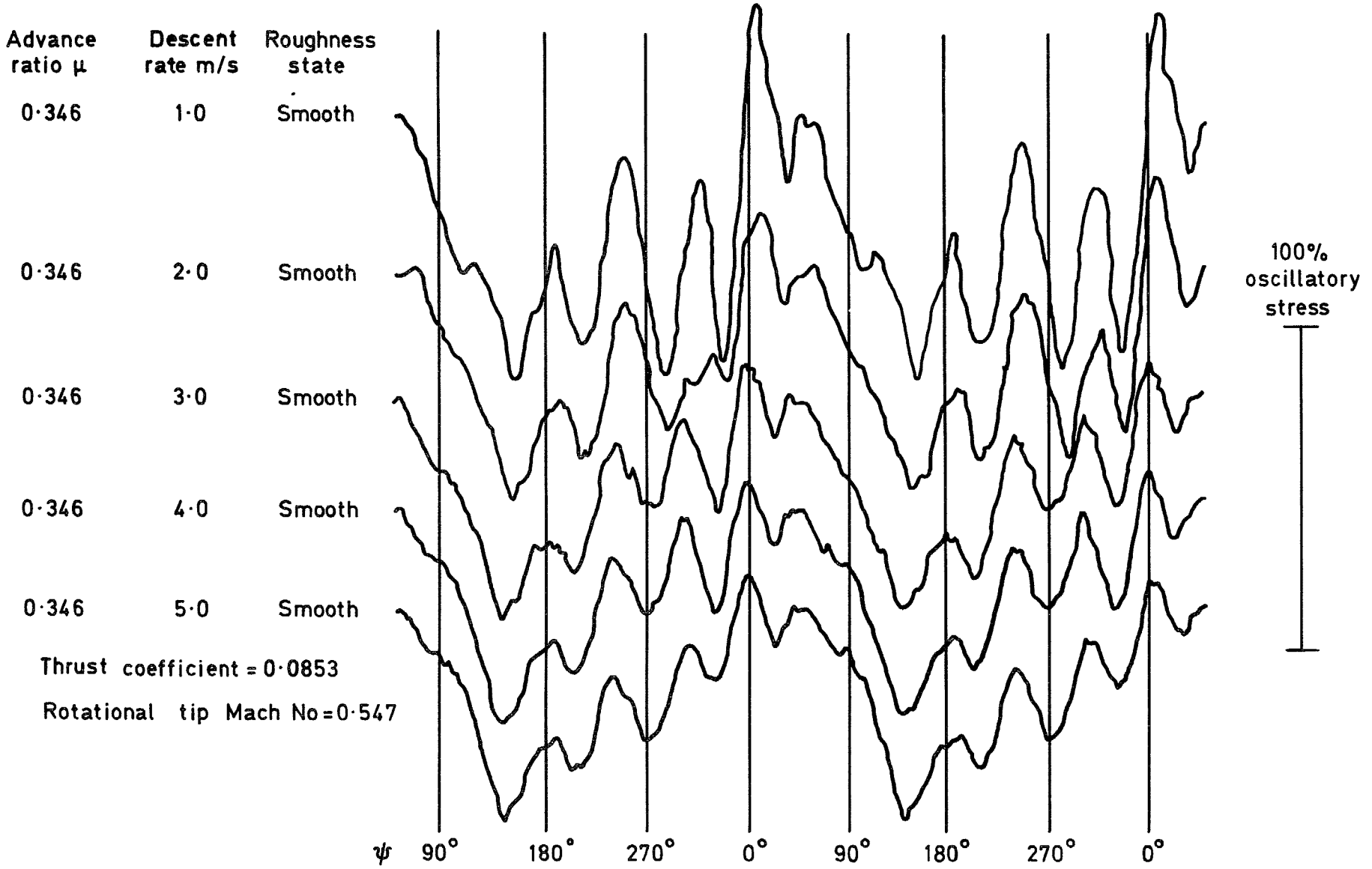

FIG. 11a. Torsional oscillation of retreating blade with unroughened blades.

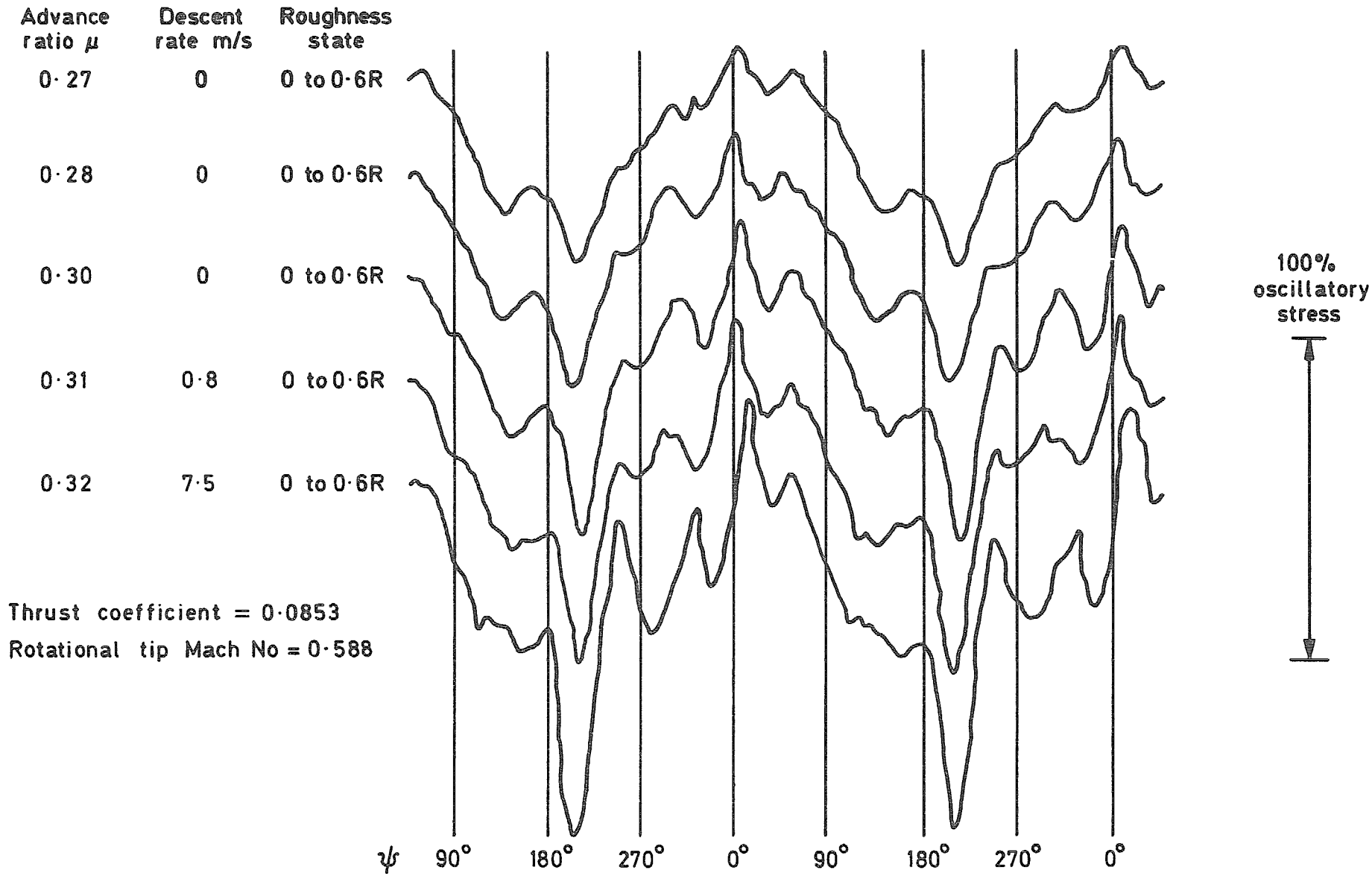

FIG. 11b. Disturbance at front of rotor disc caused by roughness from blade root to 0·6 radius.

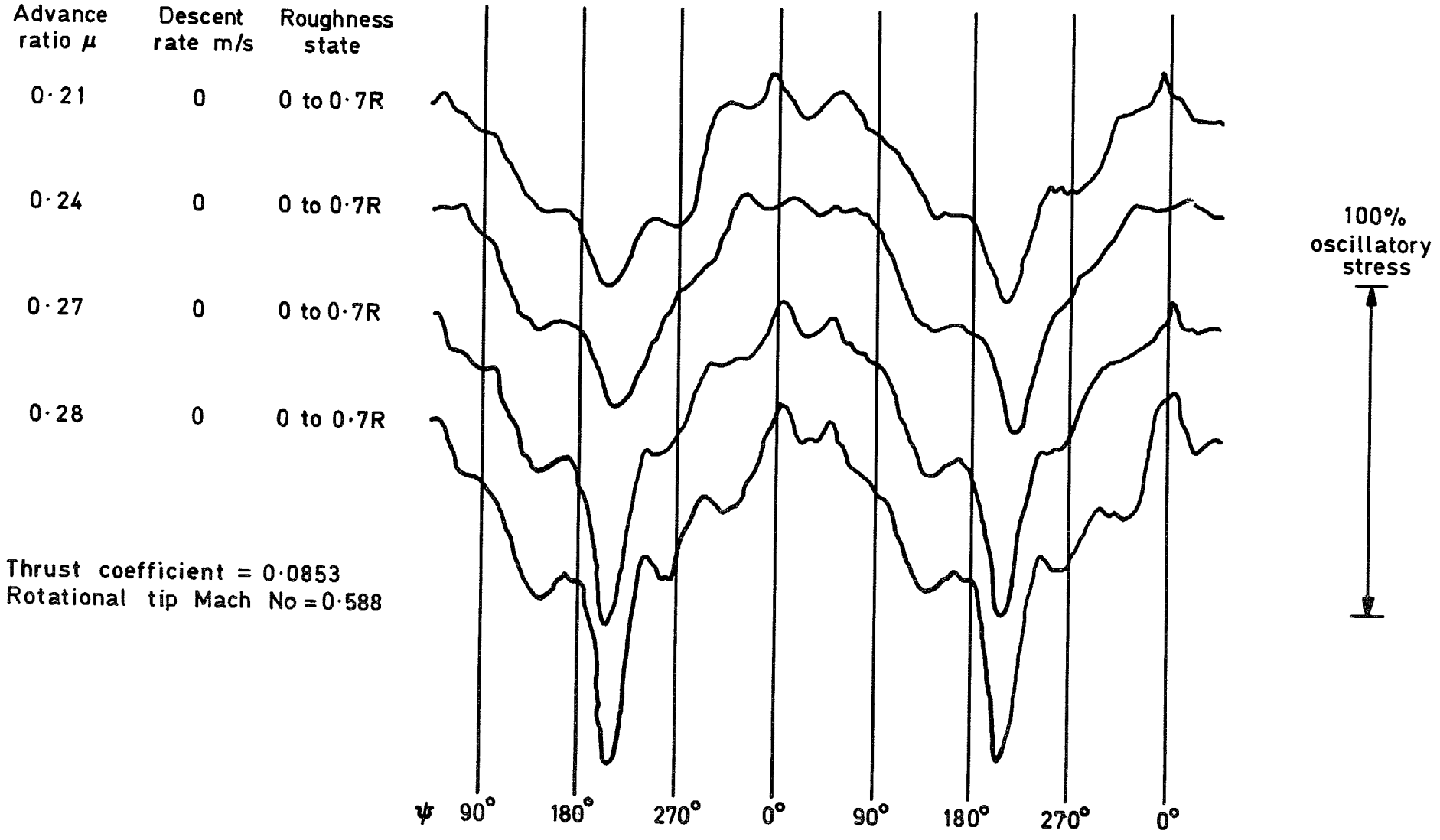

FIG. 11c. Disturbance at front of rotor disc caused by roughness from blade root to 0·7 radius.

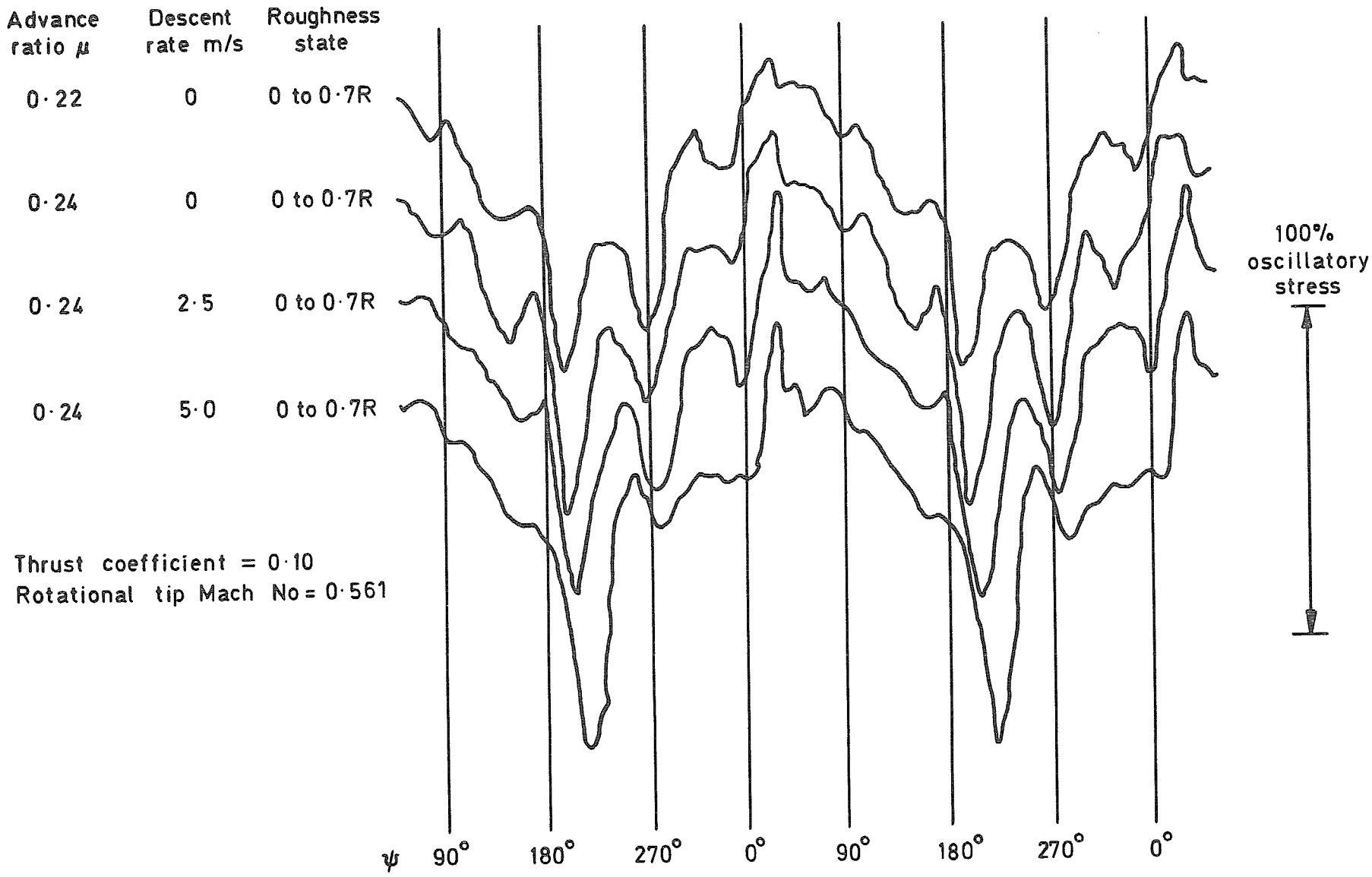

FIG. 11d. Effect of rate of descent with roughness from blade root to 0·7 radius.

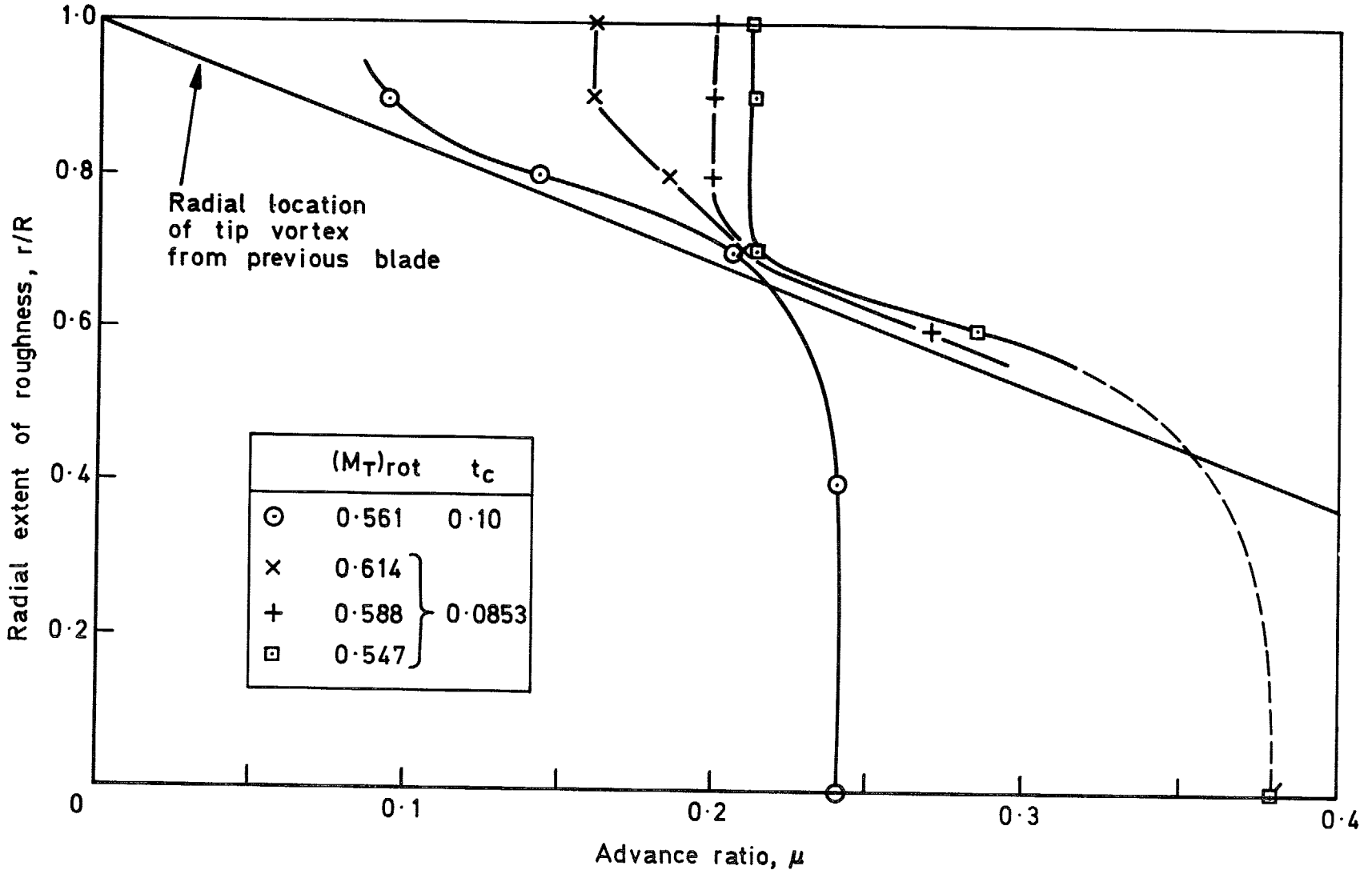

FIG. 12. The onset of the disturbance at the front of the rotor disc in level flight.

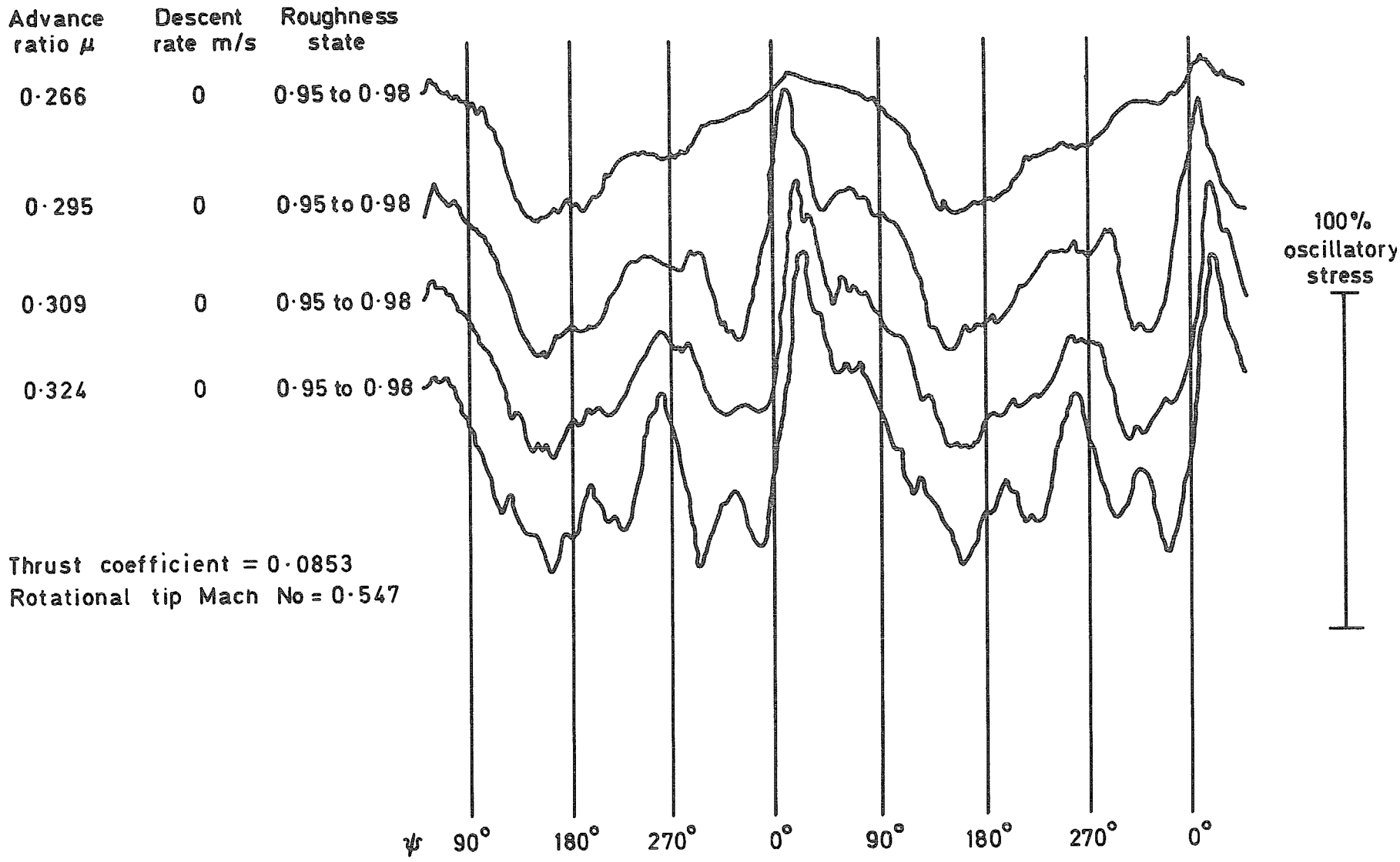

FIG. 13a. Disturbance at rear of rotor disc caused by roughness near blade tip.

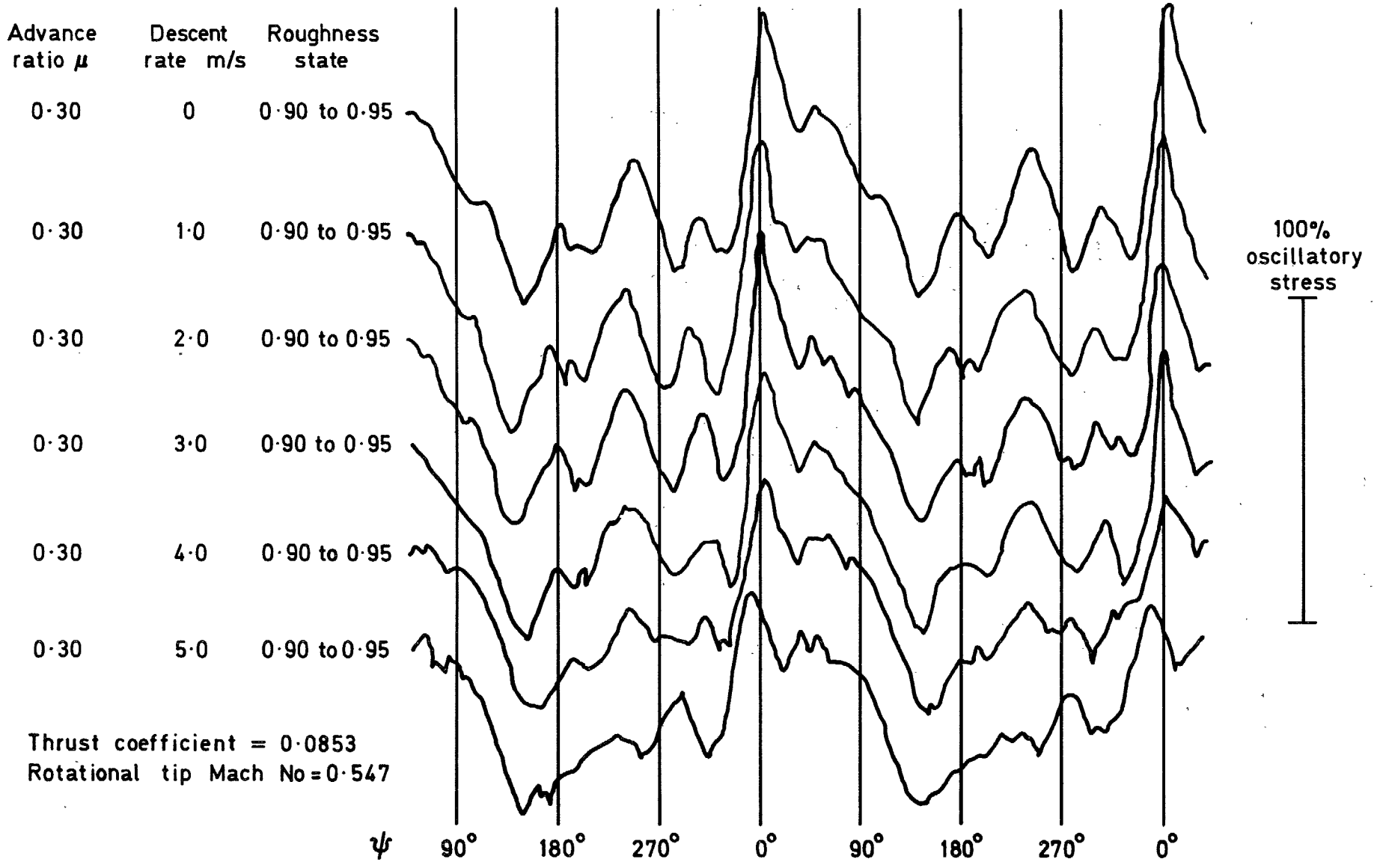

FIG. 13b. Suppression of the disturbance at the rear of the rotor disc by increasing rate of descent.

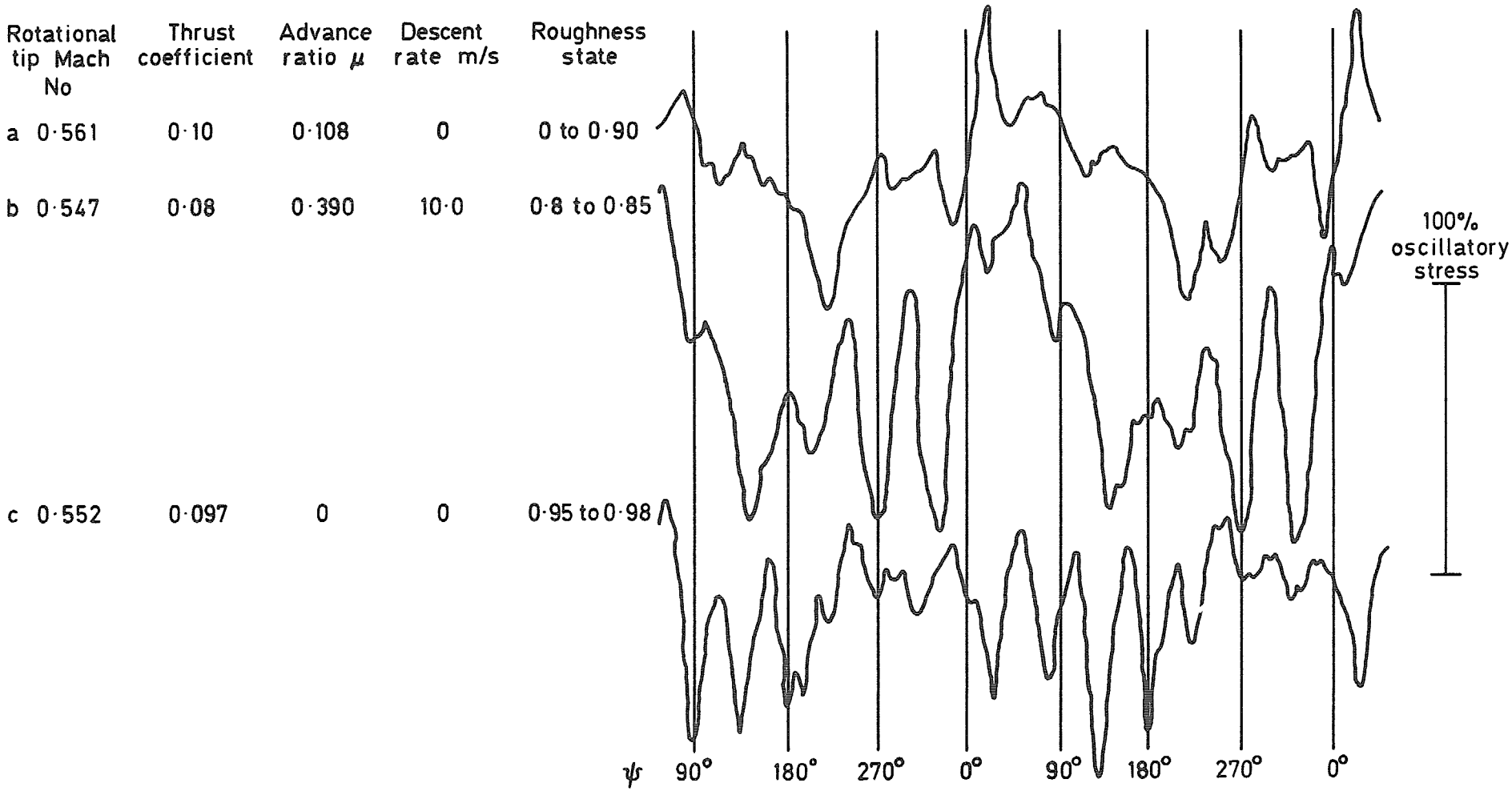

FIG. 14. Additional control load waveforms of special interest.

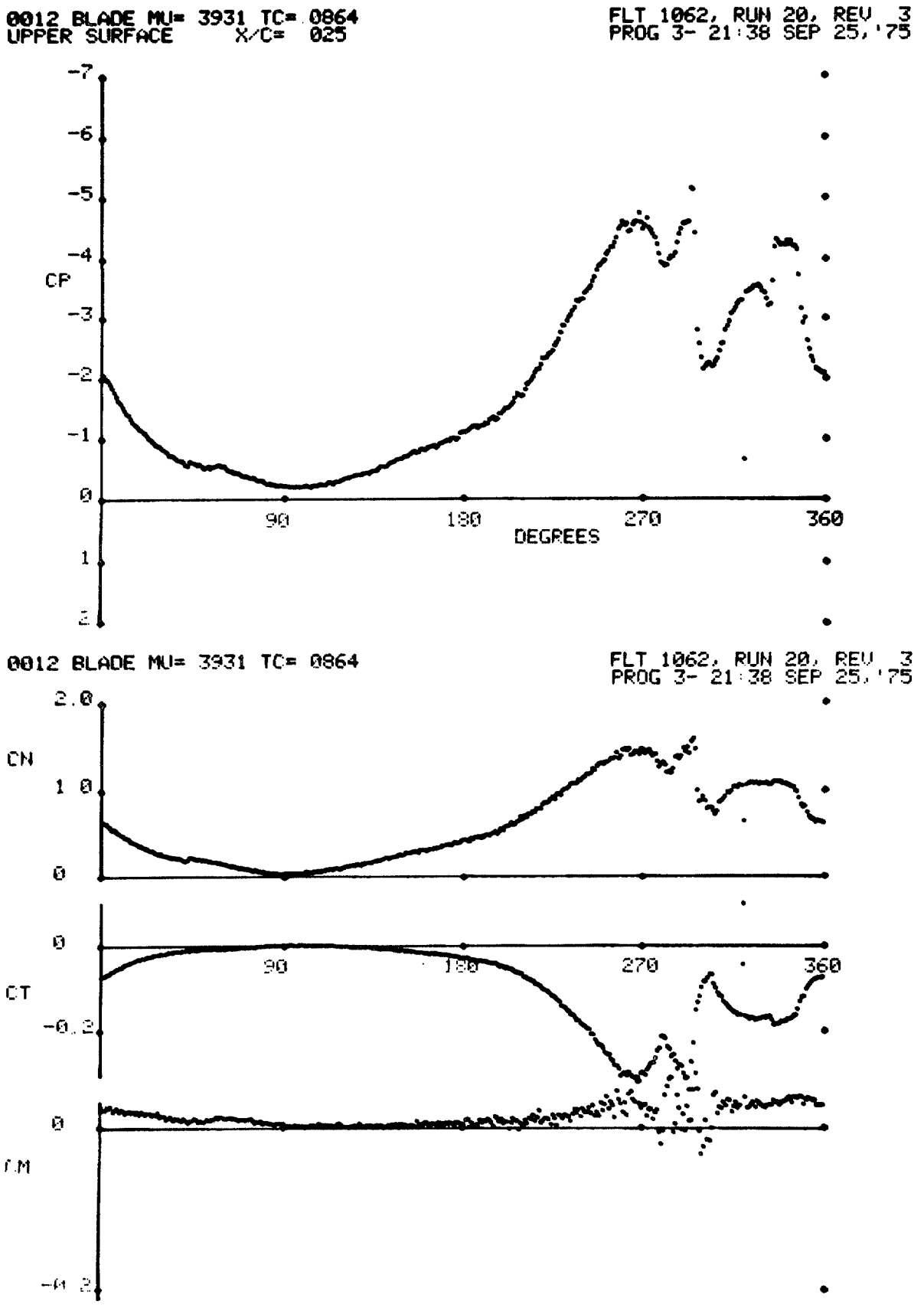

FIG. 15. Measured upper surface pressure coefficient at 0·025 chord and corresponding normal force, chordwise force and moment coefficients on modified blades.

Printed in England for Her Majesty's Stationery Office by J. W. Arrowsmith Ltd., Bristol BS3 2NT.
Dd. 587484 K.4.12/77.

First published 1978

HER MAJESTY'S STATIONERY OFFICE

Government Bookshops

49 High Holborn, London WC1V 6HB
13a Castle Street, Edinburgh EH2 3AR
41 The Hayes, Cardiff CF1 1JW
Brazennose Street, Manchester M60 8AS
Southey House, Wine Street, Bristol BS1 2BQ
258 Broad Street, Birmingham B1 2HE
80 Chichester Street, Belfast BT1 4JY

Government publications are also available through booksellers

R. & M. No. 3812
ISBN 0 11 471145 3